



## Aspects of prediction of the performance of a boiling water reactor

Petersen, T.

*Publication date:*  
1973

*Document Version*  
Publisher's PDF, also known as Version of record

[Link back to DTU Orbit](#)

*Citation (APA):*  
Petersen, T. (1973). *Aspects of prediction of the performance of a boiling water reactor*. Risø National Laboratory. Denmark. Forskningscenter Risø. Risø-R No. 289

---

### General rights

Copyright and moral rights for the publications made accessible in the public portal are retained by the authors and/or other copyright owners and it is a condition of accessing publications that users recognise and abide by the legal requirements associated with these rights.

- Users may download and print one copy of any publication from the public portal for the purpose of private study or research.
- You may not further distribute the material or use it for any profit-making activity or commercial gain
- You may freely distribute the URL identifying the publication in the public portal

If you believe that this document breaches copyright please contact us providing details, and we will remove access to the work immediately and investigate your claim.

Danish Atomic Energy Commission  
Research Establishment Risø

# Aspects of Prediction of the Performance of a Boiling Water Reactor

by Torben Petersen

August 1973

Sales distributors: Jul. Gjellerup, 87, Sølvgade, DK-1307 Copenhagen, K, Denmark

Available on exchange from: Library, Danish Atomic Energy Commission, Risø, DK-4000 Roskilde, Denmark

## Aspects of Prediction of the Performance of a Boiling Water Reactor

by

Torben Petersen

### ERRATA

Page 16,

equation (16)  $w_{e, fw} = w_{fw}(T_{fw} - T_o)C_{p, fw} + \frac{P_{fw} w_{fw}}{\rho_l}$

should read:  $w_{e, fw} = w_{fw} \int_{T_o}^{T_{fw}} C_v dT + \frac{P_{fw} w_{fw}}{\rho_l}$

equation (18)  $e_{g, sl} = h_{fg} + C_{p, sl}(T_s - T_o) - P_{sl}(\frac{1}{\rho_l} - \frac{1}{\rho_g})$

should read:  $e_{g, sl} = h_{fg} + \int_{T_o}^{T_s} C_v dT - P_{sl}(\frac{1}{\rho_g} - \frac{1}{\rho_l})$

Page 17,

equation (19)  $w_{sl} = \frac{Q_{tot}}{e_{g, sl} + \frac{P_{sl}}{\rho_{g, sl}} - \frac{P_{fw}}{\rho_{l, fw}} - C_{p, fw}(T_{fw} - T_o)}$

should read:  $w_{sl} = \frac{Q_{tot}}{e_{g, sl} + \frac{P_{sl}}{\rho_{g, sl}} - \frac{P_{fw}}{\rho_{l, fw}} - \int_{T_o}^{T_{fw}} C_v dT}$

$C_v$  is specific heat at constant volume for water

Aspects of Prediction of the Performance of a Boiling Water Reactor

by

Torben Petersen

Danish Atomic Energy Commission

Research Establishment Risø

Reactor Physics Department

Abstract

Features of the BWR-simulator complex SYNTRONVOID and ELGYFO are described. Calculations are carried out in order to demonstrate effects of various approximations in both hydraulic models and in the flux synthesis method, which is used for the neutron flux calculation. Subchannel calculations have been performed for a BWR fuel assembly to investigate effects of nonuniform radial void distribution in an assembly. Finally examples of prediction of burn out are shown.

	Page
6.2. Neutron Flux Calculation .....	59
6.3. Subchannel and Burn Out Calculations for a BWR	
Fuel Element .....	59
6.4. Conclusion .....	60
Acknowledgements .....	60
References .....	61

# CONTENTS

	Page
1. Introduction .....	5
2. The Boiling Water Reactor Simulator .....	6
2.1. The Selection of Hydraulic Models .....	7
2.2. The VOID Program .....	9
2.3. The VOIDX Program .....	13
3. Some Test Calculations with the BWR-Simulator .....	18
3.1. Selection of Parameters for the Hydraulic Models .....	18
3.2. Approximations in the Numerical Treatment of the Hydraulic Models .....	26
3.3. Concluding Remarks on the Test Calculation for the Hydraulics .....	31
3.4. The Flux Synthesis Method .....	31
3.5. Examples of Flux Synthesis Calculations for a BWR Geometry .....	33
3.6. Comparison of Flux Synthesis to Difference Equation Technique .....	39
3.7. Comparison with Nodal Theory .....	42
3.8. Concluding Remarks on the Synthesis Method .....	45
4. Subchannel Calculations .....	46
4.1. Effect of Nonuniform Void Distribution on the Power Distribution in a Dresden 1 Fuel Box .....	46
4.2. Spectrum Effects of Nonuniform Void Distribution in a Dresden 1 Fuel Box .....	51
5. Burn Out Calculations .....	52
5.1. Burn Out Correlation for SYNTRONVOID and ELGYFO ..	53
5.2. Comparisons between the Becker Correlation and General Electric Design Criterion .....	53
5.3. Burn Out Calculations by Subchannel Analysis .....	55
5.4. Concluding Remarks on Burn Out Calculations .....	57
6. Summary and Conclusions .....	58
6.1. The Hydraulic Models .....	58

## 1. INTRODUCTION

Calculation of the overall power distribution throughout the reactor core forms one of the main goals of reactor physics calculations. The ideal situation is to be able to predict the power at any point of the core at any time, since the power forms the basis of calculation of burn up and operating margins.

As in many other areas, this ideal situation does not exist. The reasons for this can be grouped in three main categories. In the first can be grouped lack of fundamental theory and data.

Fundamental data are in this connection data such as nuclear cross sections. Considering a certain nucleus, its cross section for some process can only be determined to some degree of exactness. The uncertainty can sometimes be rather great.

Lack of fundamental theory means that not all physical processes taking place in a reactor core can be described in adequate detail. As an example the boiling mechanism in a boiling water reactor can be used. The boiling mechanism is not fully understood. Instead a simple and evidently not complete model is set up. The model is then fitted to experimental data. This, of course, means a lesser generality of the model, and what is more important, it might be difficult to predict when an extrapolation by means of the model to a new situation is possible.

In the second category might be grouped fabrication tolerances and accidental and unknown changes in material and mechanical structure.

In a system like a modern power reactor, variations in mechanical dimensions and material compositions are bound to occur. The parameters of the system in hand will thus be partially unknown. In a big system, effects of such variations might cancel out each other, if one is not considering too small areas in the core. On the other hand, effects such as burn out, that is the forming of a dry patch on a fuel rod and the possibility of a subsequent destruction of the cladding are local. These might therefore be difficult to predict.

Finally, even if all data were available and if all models used were able to describe the physical situation, the total amount of data and processes is so great that a detailed calculation cannot be performed. The need for approximate methods, which calculate gross effects, is obvious. If a more detailed knowledge is required, one has to assume separability of a subsystem in the reactor in such a way that some overall calculation forms the starting point for a local calculation.

This report will emphasize a few of the above problems with special reference to boiling water reactors. It is thus approximations that arise from calculations of the steam content in the moderator which is especially considered but also some approximations in the neutron flux calculation are treated. In connection with the hydraulics calculations a procedure for calculating the burn out margin is demonstrated.

## 2. THE BOILING WATER REACTOR SIMULATOR

Unlike a pressurized water reactor an overall calculation for a BWR is bound to be three-dimensional. A PWR is controlled primarily by means of homogeneously distributed poison. The moderator density will also be almost uniform throughout the core. It is known that subcooled boiling takes place under normal operating conditions in a modern PWR. However, the homogeneously distributed absorber presumably makes the void coefficient small and the influence of boiling is small. At least experience shows that two-dimensional calculations for PWR's, assuming the power to be sinusoidal in the axial direction, seem to yield satisfactory results.

In a BWR the moderator density varies because of steam voids. These voids destroy the separability which could be assumed to exist between axial and radial power shapes in a PWR.

Consider a single fuel element. A high power production in the bottom of the element will create a strong voidage. Since the water temperature will not be far from saturation temperature, the voids will not disappear as they are streaming along the element, and thus the top of the fuel element might contain a very high fraction of steam voids without having a high power production. The same mechanism also means that the effect of the control rods is not limited to the level to which they are inserted. The control rods are inserted from the bottom of the core. A partially inserted rod will reduce the power and thereby the void production at the bottom. In this manner, the power shape will be perturbed along the whole element by the control rod.

It is thus seen that an overall calculation for a BWR involves both a three-dimensional flux calculation and a thermal hydraulic analysis.

For the first part the flux synthesis program SYNTRON<sup>1)</sup> has been used, and in order to cover the second part, the two programs VOID and VOIDX have been developed. These programs have been combined to form the two versions of a program for analysis of performance of a BWR, SYNTRONVOID and ELGYFO.

In the following VOID and VOIDX will be discussed, since the flux synthesis and the coupling between the calculation of the hydraulics and the neutron flux calculation have already been described in ref. 1 and ref. 2.

### 2.1. The Selection of Hydraulic Models

Three main thermal hydraulic factors influence the nuclear conditions in the core. These are the moderator temperature, the moderator density and the fuel temperature.

In a BWR core, the variation in coolant temperature will be rather small. It will only deviate from saturation by up to 10°C in most cases. The variations in density of the water in the water-steam mixture, which acts as moderator, will thus also be small. The steam content will exist under saturation conditions, that is the density of the steam will be almost constant and determined by the reactor pressure.

The small variation in coolant temperature also means that variations in fuel cladding temperature will be small, since it is not likely to rise more than around 10°C above the coolant temperature under normal operating conditions. The fuel temperature will therefore primarily be determined by the power dissipation of the fuel and calculation of effects of Doppler broadening in the fuel is thus almost decoupled from the hydraulics.

The conclusion is that from a nuclear point of view, the main hydraulic variable to be determined is the void fraction  $\alpha$  defined as the steam volume fraction of the steam-water mixture.

The mechanisms for heat transfer from the fuel cladding surface to the coolant and the flow of the two-phase mixture in the fuel elements are not yet fully understood, or rather, they are so complicated that no theoretical models have been set up that from basic physical laws can predict the processes taking place. If the behaviour of the coolant is to be predicted, one has to rely on experimentally fitted correlations.

Several ways of treating the problem exist. A very simple one is developed at General Electric and used in the FLARE<sup>3)</sup> program.

Considering a single fuel element, the variation in steam quality  $x$  is given by an expression of the following type

$$x_{ijl} = \left( \frac{1}{KF_{ij}} \right) \left( \sum_{k=1}^l S_{ijk} - \frac{S_{ijl}}{2} \right) (x_{ex} - x_0) + x_0 \quad (1)$$

where

$x_{ijl}$  is the steam quality in axial node l in fuel element ij

K is the number of fissions in fuel element ij

$F_{ij}$  is the ratio of flow in channel ij to the average flow

$S_{ijk}$  is the number of fissions in node ijk

$x_{ex}$  is the exit quality  $\frac{H_{exit} - H_{sat}}{H_{fg}}$

$x_o$  is the inlet quality  $\frac{H_{inlet} - H_{sat}}{H_{fg}}$

$H_{inlet}$  and  $H_{exit}$  are the inlet and exit enthalpies of the core

$H_{fg}$  is the enthalpy of evaporation.

The  $F_{ij}$ 's are determined from the polynomial

$$F_{ij} = F_{ijo} [1 + C_1 (P_{ij} - 1) + C_2 (P_{ij} - 1)^2] \quad (2)$$

where  $P_{ij}$  is the power of channel ij and  $C_1$  and  $C_2$  are constants, which are determined outside the FLARE program.

Throughout this report the steam quality will normally be defined as

$$x = \frac{w_g}{w_g + w_f} \quad (3)$$

where

$w_g$  is the mass flow rate of steam

$w_f$  is the mass flow rate of water.

However, in (1) x is defined as

$$x = \frac{H - H_{sat}}{H_{fg}} \quad (4)$$

where

H is the actual enthalpy of the coolant

$H_{sat}$  and  $H_{fg}$  are the same as before.

If no boiling took place below saturation,  $x \leq 0$  would be a direct measure of liquid subcooling and if all heat supplied to the coolant as it had reached saturation went into evaporation  $x > 0$  again would be the steam volume fraction.

This is of course not the true picture of the situation. In order to transfer heat from the wall of the fuel cladding to the coolant, the wall temperature has to be higher than the coolant temperature. Thus the wall will reach saturation temperature before the coolant. As soon as this happens, boiling will start at the heated surface, that is subcooled boiling takes place. A void fraction greater than 0 should therefore be allowed, even if  $x \leq 0$  in (1).

In fact, the void fraction in the FLARE model is calculated from

$$\begin{aligned} \alpha &= R_1 + R_2 x + R_3 x^2 - R_4 e^{\left(\frac{R_5 - x}{R_6}\right)} & \text{for } x > R_5 \\ \alpha &= 0 & \text{for } x < R_5 \end{aligned} \quad (5)$$

where the polynomial coefficients  $R_1, R_2, \dots$  are found from experimental data. By proper choice of  $R_5$ , subcooled boiling can be taken care of.

The model is attractive since it is very convenient to a computer program. However, when experimental correlations are used, one should be extremely careful only to use them in the areas where the original experimental results stem from. Furthermore, the cruder the model, the more sensitive it might be to conditions for which it can be used.

It has therefore been decided to use a more detailed set of models. More detailed in the sense that the different processes taking place are separately taken care of. In this manner it was believed that a more generally useable and flexible tool could be developed.

The models used were originally developed for the Ramona<sup>4)</sup> program. A description is found in ref. 4. The actual use of the models is described in ref. 2.

The models include models for subcooled boiling, for bulk boiling and condensation, slip, single phase and boiling heat transfer.

## 2.2. The VOID Program

A BWR core consists of a number of fuel elements surrounded by a shroud. The flow along a single fuel element is therefore isolated from the rest of the core. Only heat conduction across the shroud and the part

of the energy released as  $\gamma$ -energy, form direct connections to the surroundings in the core. The fuel elements will in the following be named coolant channels, when hydraulic features are considered.

The water flowing between the coolant channels will only receive heat from heat conduction across the shrouds and  $\gamma$ -energy. It is treated as a single channel, named the moderator channel. A schematic diagram of the core is shown in fig. 2.2. a.

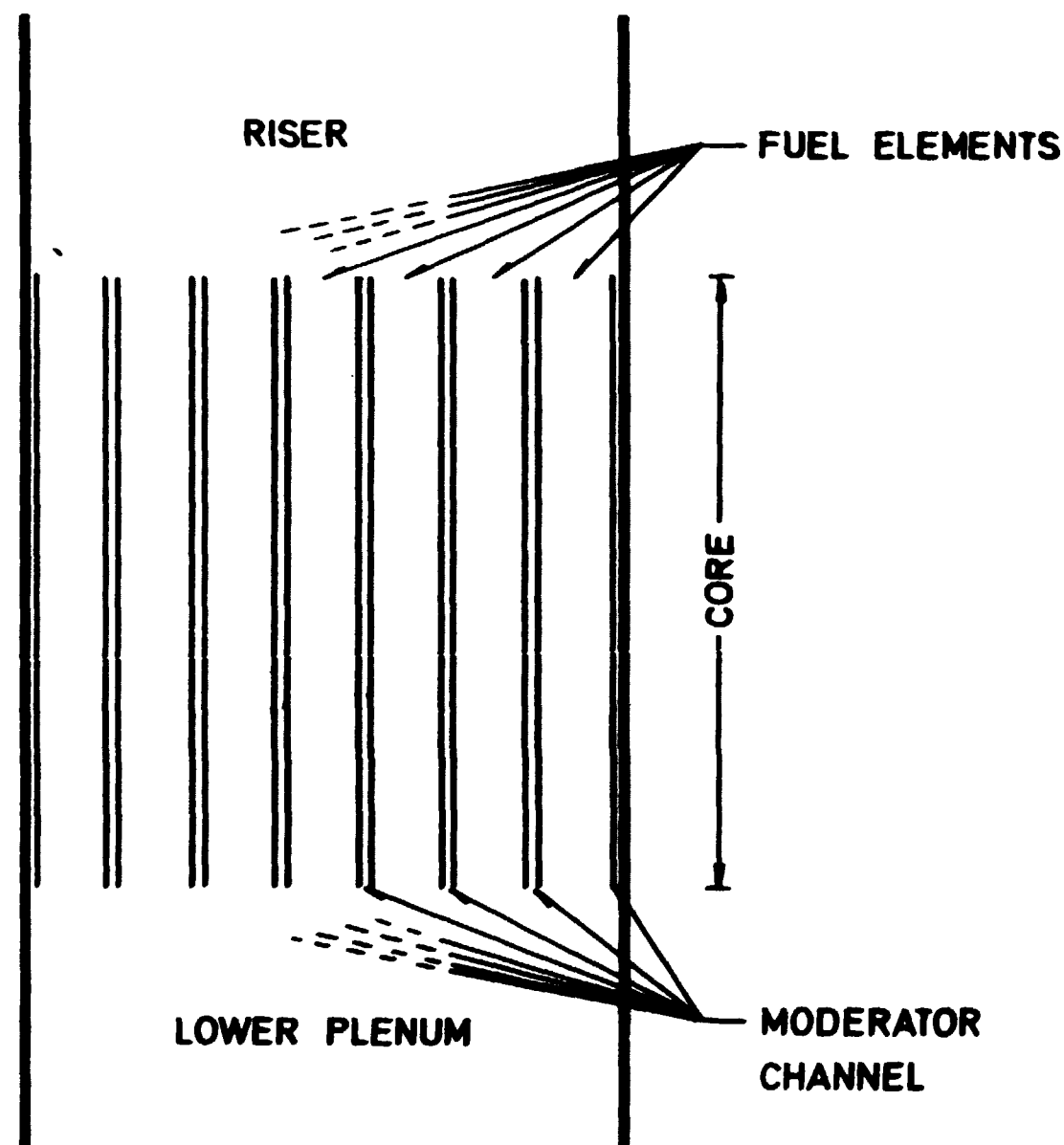


Fig. 2.2a. Schematic diagram of the core configuration in the VOID program.

The flows to all coolant channels and the moderator channel are supplied from the lower plenum at the bottom of the core. At the top all flows are mixed in the riser section. Both in the riser and in the lower plenum, zero transverse pressure drop is assumed. The flows should therefore be distributed to the channels according to the conditions

$$\Delta p_i = \Delta p_j \quad \text{for } j, i = 1, 2, \dots, N \quad (6)$$

and

$$w_0 = \sum_{i=1}^N w_i \quad (7)$$

where

$\Delta p_i$  and  $w_i$  are pressure drop and mass flow rate channel  $i$  respectively

$N$  is the number of channels including the moderator channel

$w_0$  is the total mass flow rate for the core.

In the VOID program  $w_0$ , the pressure at the inlet of the core and the inlet subcooling should be given.

The program then adjusts the  $w_i$ 's to satisfy (6) and (7). This is accomplished by a very simple iterative procedure. A guess on the  $w_i$ 's are performed and the  $\Delta p_i$ 's are calculated. A new value of the  $w_i$ 's is guessed and a new set of  $\Delta p_i$ 's calculated. From now on, new values are found from

$$w_i = w_i' + d_i (\Delta p_i' - \Delta p) \quad (8)$$

where

$$d_i = \frac{w_i' - w_i''}{\Delta p_i' - \Delta p_i''} \quad (9)$$

The primed and double-primed values stem from the two preceding iterations.

By selecting

$$\Delta p = \frac{\sum_{i=1}^N \Delta p_i' d_i}{\sum_{i=1}^N d_i} \quad (10)$$

(7) is automatically satisfied, if (6) is satisfied by the preceding iteration.



The  $\Delta p_i$ 's are a sum of pressure drops due to friction, gravitation and acceleration (ref. 2). In order to calculate these, one has to know the steam quality distribution. Finding the flow distribution involves several calculations of the  $\Delta p_i$ 's. If the number of channels are great, and the detailed models for the hydraulics of the channels are used, the computing time for this will become rather great. Instead calculation of flow distribution and calculation of void distribution in the channels have been separated.

During the iterations for finding the  $w_i$ 's, the  $\Delta p_i$ 's are calculated by a model somewhat similar to the FLARE model.

At the bottom of the channels, it is assumed that all heat is used for heating the liquid, and no boiling takes place. When the water temperature has risen to a temperature  $T$  for which

$$q'' > k (T_s - T) \quad (11)$$

where

$q''$  is the heat flux

$k$  is the single phase heat transfer coefficient

$T_s$  is the saturation temperature

boiling is assumed to start. From this point the steam quality  $x$  is given by

$$x = \frac{Q}{Q_0} x_{ex} \quad (12)$$

where

$Q_0$  is the integrated power of the fuel element from the point, where boiling sets in, to the top.

$Q$  is the integrated power from the point, where boiling sets in, to the actual point.

$x_{ex}$  is the exit steam quality.

When the  $w_i$ 's are found, the detailed models are used for finding the void distribution in the channels.

At first  $x_{ex}$  has to be guessed, but since the determination of a static picture of a BWR core involves several iterations between hydraulic calculations and power calculation,  $x_{ex}$  from the preceding hydraulic calculation can be used.

The void fraction for the pressure drop calculation is obtained from (12) by using the same slip model as the detailed calculation.

This simple model predicts the steam quality in the upper part of the

channels rather well. Since  $x$  is increasing along the channels,  $x$  will be biggest at the top. The steam content will be best predicted for the area, where the effects on the pressure drop of the coolant being a two-phase mixture are greatest. In addition, a throttling is normally found in the inlet of the fuel elements. This yields normally the greatest part of the total pressure drop across the fuel element. Since there is no steam at the inlet, the pressure drop across the throttling can be calculated correctly.

Thus the accuracy of the pressure drops and thereby the  $w_i$ 's calculated by the simple model should be satisfactory.

Several tests, comparing the approximate method with the detailed calculation, have been carried out for core configurations with few channels. In the test examples,  $x_{ex}$  has been in the range from 2% - 15%. Configurations with varying channel power have been used and the throttling at the inlet was in the range 20 - 60 velocity heads. (Pressure drop across singularities is calculated from  $\Delta p = 1/2 L \rho v^2$ , where  $\rho$  is the density of the coolant,  $v$  is the velocity and  $L$  is the loss in velocity heads).

In all cases the difference in void fraction was less than 1.5% and the power shapes deviated less than 0.75% compared to the detailed model.

The computing time also seems to be satisfactory. For typical calculations, the hydraulic calculation uses around 10% of the total computing time of a static picture of a BWR core.

### 2.3. The VOIDX Program

The VOIDX program is an extension of the VOID program. It contains the same model for the reactor core, and in addition a model for the rest of the cooling circuit.

A diagram of the system is shown in fig. 2.3a. This geometry is in the program represented by the geometry shown in fig. 2.3b.

From the upper plenum the flow goes down into downcommer 1 and then into downcommer 2. The downcommers might have different flow cross section and also different angles to vertical.

From the downcommers the flow continues to lower plenum 1, in which the flow is horizontal, and to lower plenum 2 where the flow is vertical upwards. Then the flow is distributed in the core, and having passed this, mixes again in the riser, which is also vertical. Finally it enters the upper plenum.

In downcommers and lower plena boiling is not allowed. In the riser bulk boiling and condensation are described by the same models as in the

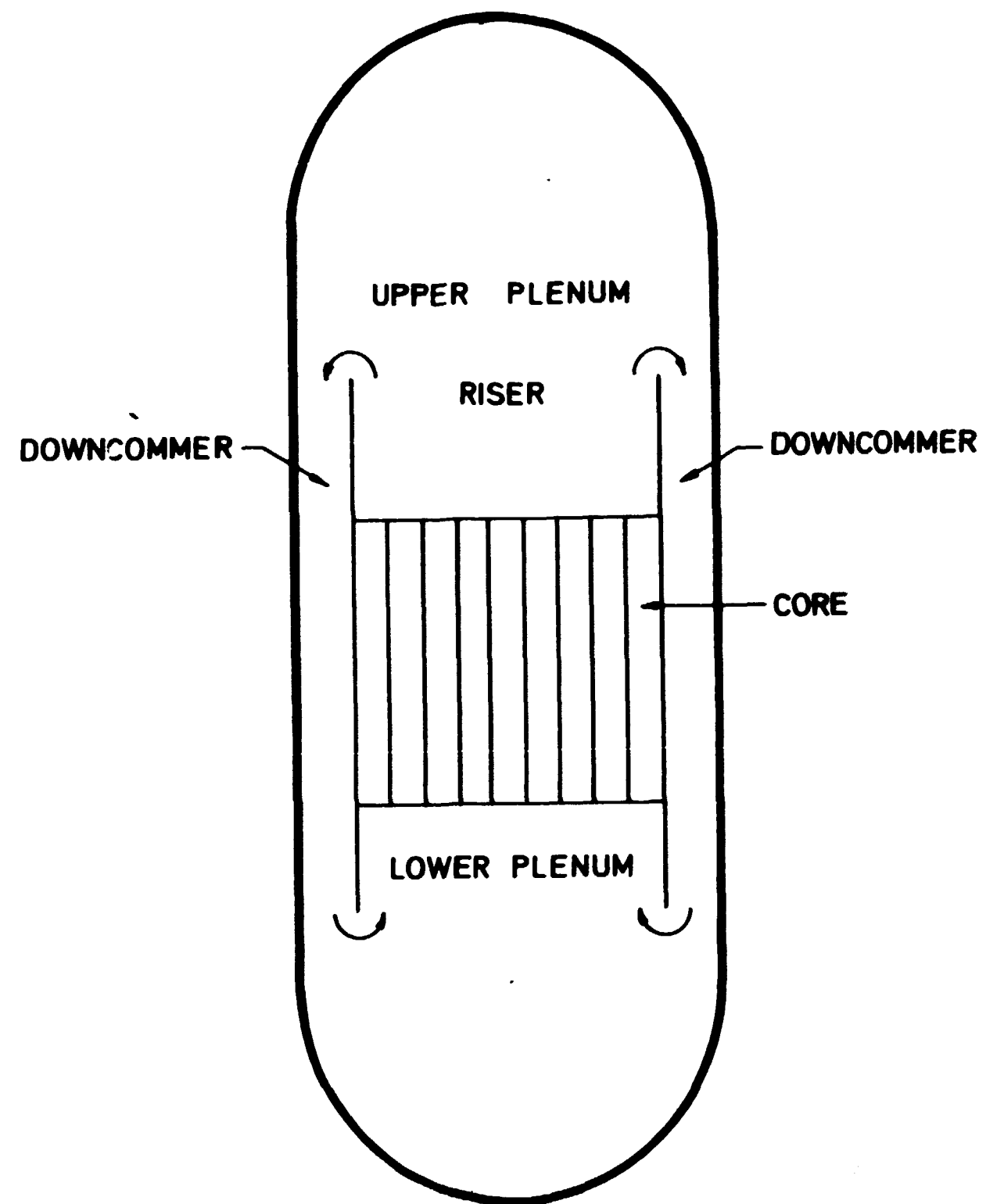


Fig. 2.3a. Cross section of BWR pressure vessel.

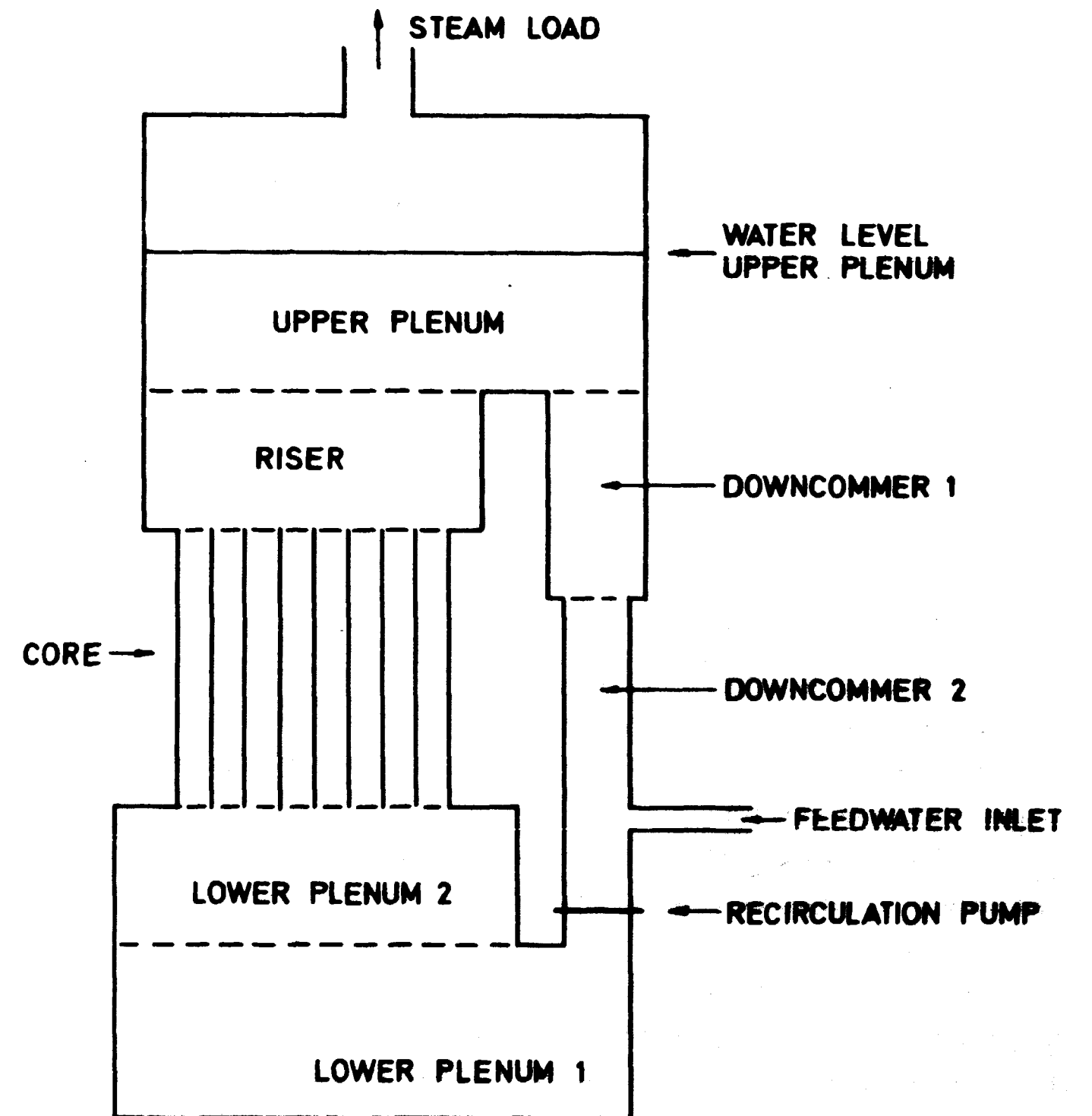


Fig. 2.3b. Schematic diagram of BWR coolant circuit used in VOIDX.

core. A slip model similar to that used in the core is also used here.

In the upper plenum boiling and condensation are described as in the riser, but the same slip formalism is not used, since no liquid flow is calculated in the upper plenum. The steam is assumed to move upwards with the same velocity as in the exit of the riser. The steam content is assumed to be uniformly distributed in the horizontal plane throughout the upper plenum.

Pressure drops in the outer coolant loop are as before a sum of pressure drops due to friction, gravitation and acceleration. As in the core the friction is calculated by means of the equivalent diameter concept. Singularities, as f. ex. transition between different flow areas, have to be given in velocity heads.

A recirculation pump may be placed anywhere in downcomers or lower plenum. Its pump head is given by

$$\Delta p = C_0 + v C_1 + C_2 v^2 \quad (13)$$

where

$v$  is the coolant velocity

$C_0$ ,  $C_1$  and  $C_2$  are constants.

All steam which reaches the top of the upper plenum leaves the coolant loop and goes to the turbine. When the steam leaves the system, it is assumed to be at saturation.

The flow of water, which leaves the system as steam, reenters as feed water. It might be entered anywhere in upper plenum, downcomers or lower plenum.

The outer parameters, determining the state of the system, are now the pressure above the upper plenum, water height in upper plenum, pump characteristic, total thermal power of the reactor and feed water temperature. Using the above assumptions, steam load is found from an overall plant heat balance. One has

$$w_{fw} = w_{sl} \quad (14)$$

$$Q_{tot} = w_{e,sl} - w_{e,fw} \quad (15)$$

$$w_{e,fw} = w_{fw} (T_{fw} - T_0) C_{p,fw} + \frac{P_{fw} w_{fw}}{\rho_1} \quad (16)$$

$$w_{e,sl} = w_{sl} e_{g,sl} + P_{sl} \frac{w_{sl}}{\rho_g} \quad (17)$$

$$e_{g,sl} = h_{fg} + C_{p,sl} (T_s - T_0) - P_{sl} \left( \frac{1}{\rho_1} - \frac{1}{\rho_g} \right) \quad (18)$$

where

$w_{fw}$  is feed water flow

$w_{sl}$  is steam load

$Q_{tot}$  is total reactor thermal power

$w_{e,fw}$  is energy flow in feed water given by (16)

$w_{e,sl}$  is energy flow to steam load given by (17) and (18)

$T_{fw}$  is feed water temperature

$T_s$  is saturation temperature

$T_0$  is some arbitrary reference temperature

$p$  is pressure

$C_p$  is specific heat at constant pressure

$h_{fg}$  is enthalpy of evaporation

$\rho_1$  and  $\rho_g$  are water and steam densities, respectively.

Equations (14) to (18) are combined to give

$$w_{sl} = \frac{Q_{tot}}{e_{g,sl} + \frac{P_{sl}}{\rho_{g,sl}} - \frac{P_{fw}}{\rho_{1,fw}} - C_{p,fw} (T_{fw} - T_0)} \quad (19)$$

In the upper plenum no liquid flow was calculated and the pressure drop between the outlet of the riser and the inlet of downcommer 1 is neglected.

The flow rates in the system can then be determined from the condition.

$$\Delta p_{d1} + \Delta p_{d2} + \Delta p_{lp1} + \Delta p_{lp2} + \Delta p_{pump} + \Delta p_{core} + \Delta p_{riser} = 0 \quad (20)$$

$$\Delta p_i = \Delta p_{core} \quad i = 1, 2, \dots, N \quad (21)$$

where

$\Delta p$  is the pressure drop across the different parts of the loop

$\Delta p_i$  is pressure drop across the  $N$  channels in the core.

The procedure for finding the flow rates in VOIDX is an extended version of the one described for VOID.

Input sheets and a description of the structure of the programs SYNTRONVOID and ELGYFO will be given in a future report.

### 3. SOME TEST CALCULATIONS WITH THE BWR SIMULATOR

In the above chapter the argument for using a rather detailed set of hydraulic models, which will require more computing time than a simple model, as that it would be more generally valid. However, even the detailed models do not describe the physical processes only in terms of natural constants but they also contain fitted parameters. Their validity can thus only be established through comparison with experiment.

It has been shown<sup>4, 5)</sup> that the models can be fitted to describe experimental situations. In order to show general validity, models correlated for one experiment should be used for another experiment. The calculations for the Dresden 1 reactor<sup>2)</sup>, for which constants for the hydraulic models have been taken from ref. 4, yielded reasonable results. It seems to be possible to select constants from cases similar to that in hand and to get satisfactory results.

This conclusion cannot of course be drawn from one example. Also the number of approximations in an overall calculation is very great and these might cancel out each other. To illustrate the problems some calculations for the Dresden reactor is summarized in the following.

#### 3.1. Selection of Parameters for the Hydraulic Models

In this section some selected calculations for a quarter core of the Dresden 1 reactor are shown in order to demonstrate the effects of different parameters for the hydraulic models. The core configuration and control rod setting are shown in fig. 3.1a. The number of nodes, the control rods are inserted from the bottom of the core is shown. Each of the coarse meshes shown in fig. 3.1a represents four fuel elements associated a control rod position. In fig. 3.1a is also shown the numbering of the hydraulic channels. The main data of the core are found in table 3.1a.

The calculations are carried out by means of SYNTRONVOID. The nuclear data used are those for hot clean condition of the core<sup>2)</sup>.

The three main results of interest from an overall calculation will be power shape, total multiplication factor  $k_{eff}$  and steam void fraction or steam quality.

Previously it has been shown that the main hydraulic parameter determining the nuclear performance of the core is the void fraction. Only those models which primarily determine the void fraction will therefore be considered. From ref. 2 it is recalled that these are firstly the models for

8		10		5	
	10		7		
	5				
10		10			

Dresden 1, quarter core. Control rod setting for test of hydraulic models.

1	2	5	6	7	8
3	4	13	14	15	16
9	17	21	22	23	24
10	18	25	26	27	
11	19	28	29		
12	20	30			

Numbering of hydraulic channels in Dresden 1.

Fig. 3.1a.

Table 3.1a

Heat output (MW)	620
Net elect. (MW)	180
Active core height (cm)	275.4
Equivalent diameter (cm)	326
Fuel enrichment (w/o U <sup>235</sup> )	1.5
Number of fuel boxes max.	488
Number of rods in each box	36
Number of cruciform control rods	80
Fuel element pitch (cm)	12.65
Fuel rod pitch (cm)	1.8034
Fuel rod outside diameter (cm)	1.448
Fuel rod zircaloy-2 cladding thickness (cm)	0.0762
Fuel pellet diameter (cm)	1.255
Moderator temperature (°C)	284
Average clad temperature (°C)	294
Average fuel temperature (°C)	541
Average power density in core (W/cm <sup>3</sup> )	31.2
Average power density (W/cm rod)	143.0
Connector length (cm)	4.45
System pressure (bar)	69
Total mass flow rate (kg/s)	4.764 · 10 <sup>3</sup>
Inlet subcooling (°C)	21.8
Pressure drop across the core (bar)	0.53
Coolant channel flow area (cm <sup>2</sup> )	61.50
Coolant channel hydraulic diam. (m)	0.001444
Moderator channel flow area (m <sup>2</sup> )	1.691
Moderator channel hydraulic diam. (m)	0.02199
Shroud perimeter (m)	0.4420
Fuel pin perimeter per channel (m)	1.6174
Channel height (m)	2.7535

boiling, consisting in a model for steam generation at the heated surface and a model for bulk boiling and condensation. Only the last contains fitted constants. The total boiling rate  $\Psi$  is given by

$$\Psi = \Psi_{sf} + \Psi_B \quad (22)$$

where

$$\Psi_B = \frac{V}{h_{fg}} (R_0 + R_1 \alpha(1-\alpha))(1-\alpha)(T-T_s) \quad \begin{cases} + & \text{for } T > T_s \\ - & \text{for } T < T_s \end{cases} \quad (23)$$

and where

$V$  is the volume of the boiling mixture

$h_{fg}$  is enthalpy of evaporation

$\alpha$  is the steam void fraction

$T$  is the temperature of the liquid

$T_s$  is the saturation temperature

$R_0$ ,  $R_1$  and  $\alpha$  are fitted constants.

Secondly the slip model plays an important role in determining the void fraction

$$v_g = S v_f + S_g \quad (24)$$

$$S = S_1 + S_2 \alpha^r \quad (25)$$

where

$v_g$  is the velocity of the steam

$v_f$  is the velocity of the water

$S_1$ ,  $S_2$ ,  $r$  and  $S_g$  are fitted constants and  $S_g$  is that part of the steam velocity which originates from buoyancy.

As a starting point for the calculations has been chosen the values which were used in the calculation for the Dresden reactor in ref. 2. These were

$$\begin{aligned} R_0 &= 5 \cdot 10^6 & R_1 &= 4 \cdot 10^7 & \alpha &= 0.85 \\ S_1 &= 1.0 & S_2 &= 0 & S_g &= 0.91. \end{aligned}$$

From the starting values the parameters have been changed within reasonable limits, set by experience with the models from elsewhere.

It has not been intended to carry out a full parameter study. Attempts

have been made to stress the general trends only. In addition every case represents a considerable computing time and therefore only a few calculations have been carried out. In table 3.1b the obtained  $k_{eff}$ 's are shown and fig. 3.1b, fig. 3.1c, fig. 3.1d and fig. 3.1e show the power shape and void distribution of channel 17, which contains a half inserted control rod.

Table 3.1b

$R_0$	$R_1$	$\alpha$	$S_1$	$S_2$	$S_g$	$k_{eff}$
$5 \cdot 10^6$	$4 \cdot 10^7$	0.85	1.0	0	0.914	1.00295
$2 \cdot 10^7$	$4 \cdot 10^7$	0.85	1.0	0	0.914	1.00867
$5 \cdot 10^6$	$10^8$	0.85	1.0	0	0.914	1.00737
$5 \cdot 10^6$	$4 \cdot 10^7$	0.85	1.3	0	0	1.00253
$5 \cdot 10^6$	$4 \cdot 10^7$	0.85	1.4	0	0	1.00502

If the power shapes for different values of the constants for the boiling model are considered, it is seen that even a considerable change in these changes the power shape less than 10%.

A great change in slip will change the power shape considerably. A higher slip will yield a lesser void fraction and the power shape will move towards the unvoided shape. The power peak will therefore move upwards.

However, for normal reactor configurations the total slip  $S$  is known to be around 1.3 - 1.4. Within this range in slip value, the change in power shape is not great.

It is thus seen that if one has no direct knowledge of the system in hand, the constants for the hydraulic models might be selected to yield power shapes, for which the uncertainty, due to these constants, is less than 10%.

Considering  $k_{eff}$  a variation of around 0.5% is found. This is not a great change, but since reactor configurations for which reactor calculations normally are performed almost always have  $k_{eff} = 1$ , one might be tempted to adjust some hydraulic parameter to yield this value. In a complicated calculation for a reactor it is difficult to decide what should be adjusted.

NO. OF AXIAL NODES FROM BOTTOM

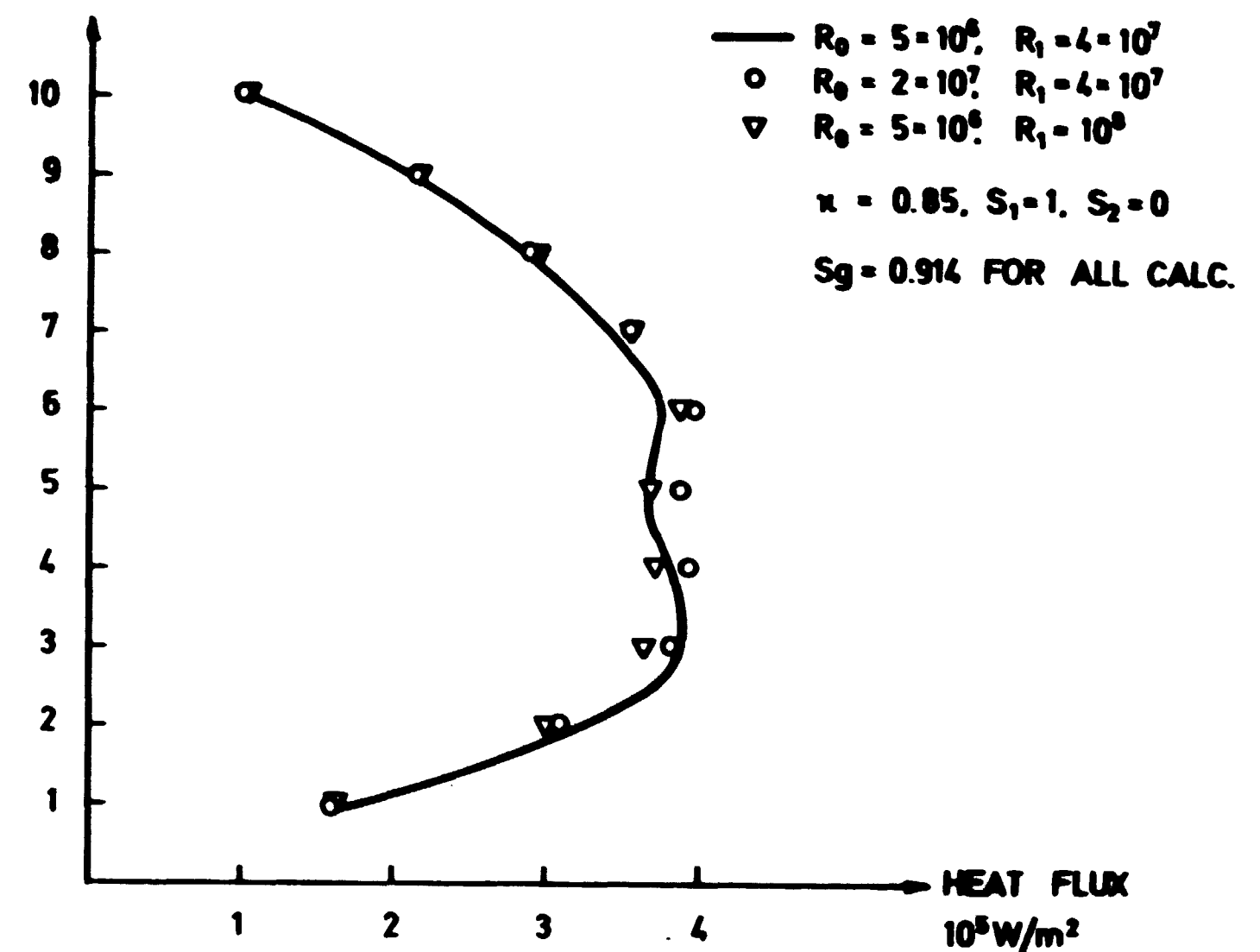


Fig. 3.1b. Power shape channel 17. Test of influence of hydraulic models. Boiling model.

It might be impossible to detect whether the representation of control rods should be altered or the value of the slip should be changed.

As long as the calculation yields  $k_{eff}$  almost equal to 1, the calculated value is not very important since it is known to be 1. Normally it is only of interest to calculate reactivity changes.

Undesirable changes in power shape, even if they are small, should therefore not be introduced by altering some parameter, if this is not justified by any other reason than  $k_{eff}$  should be equal to 1.

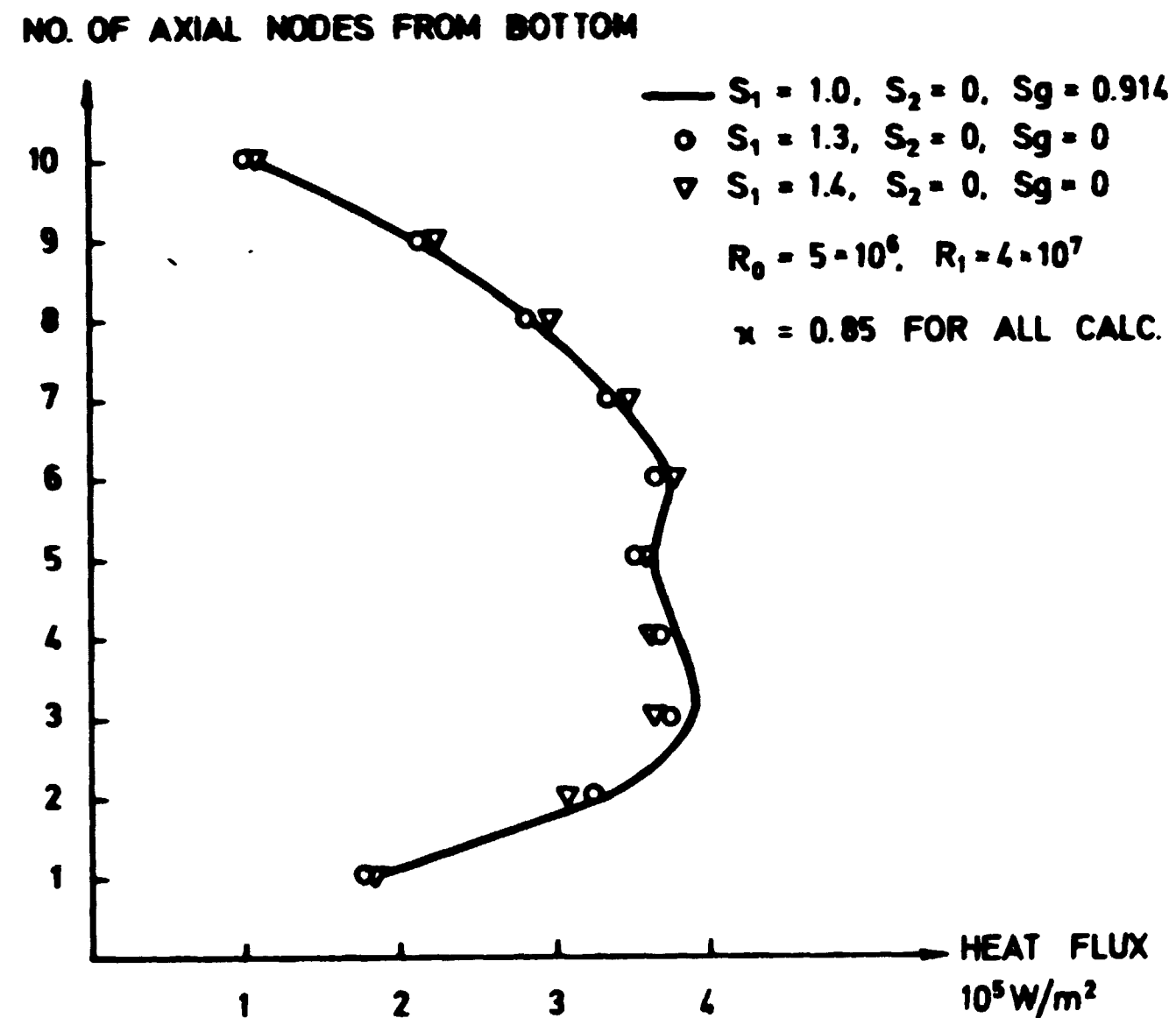


Fig. 3.1c. Power shape channel 17. Test of influence of hydraulic models. Slip model.

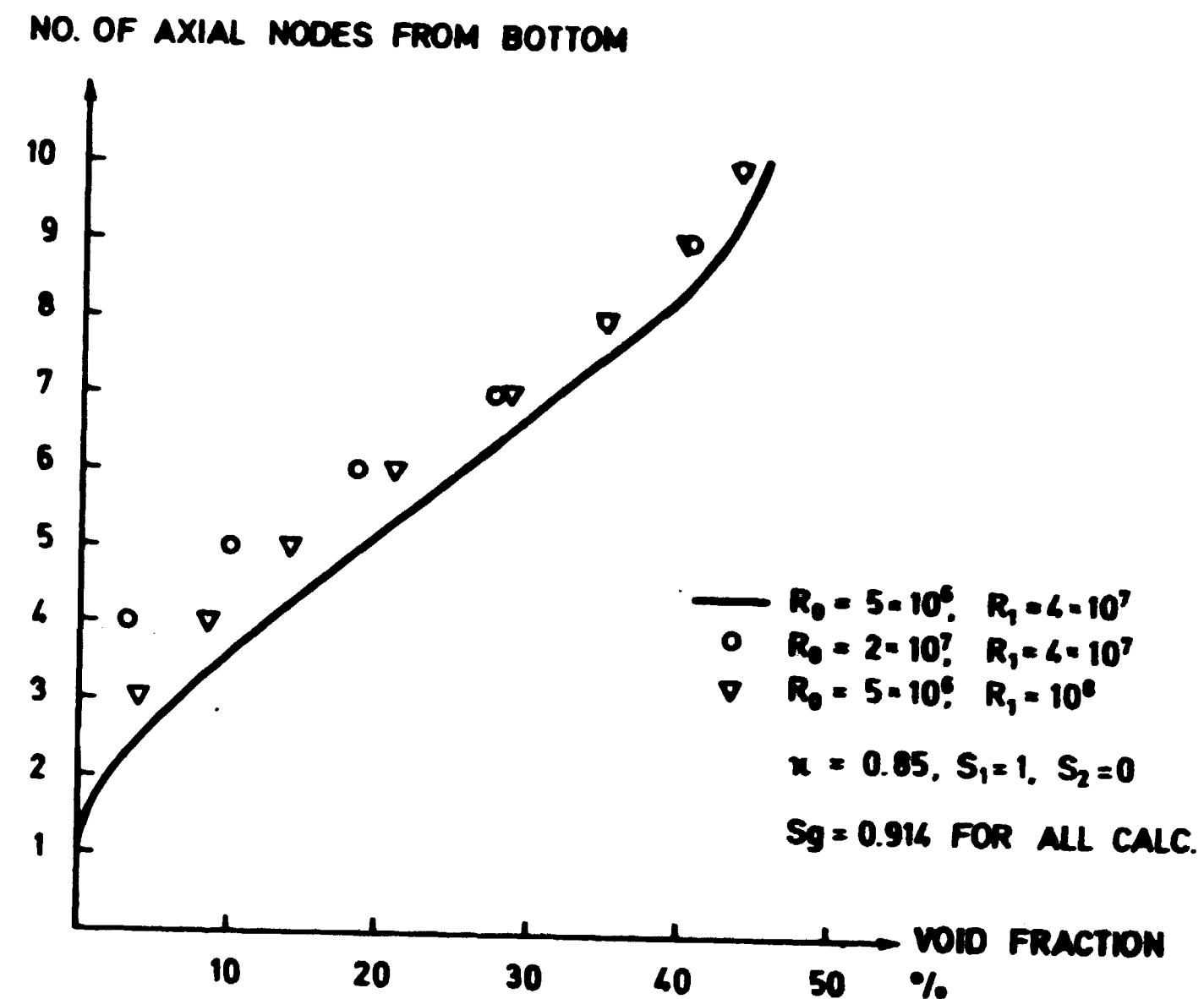


Fig. 3.1d. Void distribution channel 17. Test of influence of hydraulic models. Boiling model.

# NO. OF AXIAL NODES FROM BOTTOM

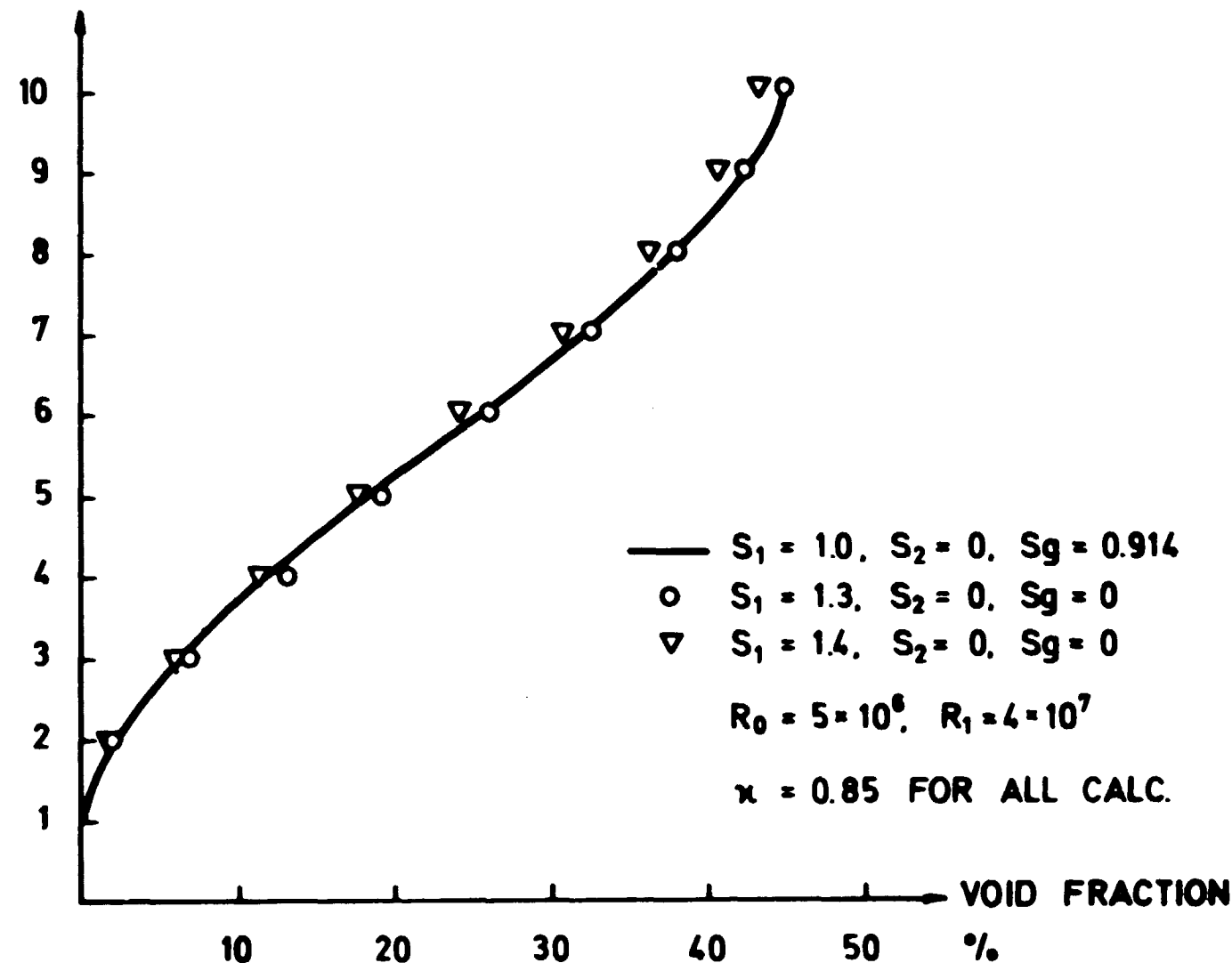


Fig. 3.1e. Void distribution channel 17. Test of influence of hydraulic models. Slip model.

## 3.2. Approximations in the Numerical Treatment of the Hydraulic Models

Until now some of the problems concerning the physical models for the coolant in a boiling water reactor core have been discussed.

When calculations are carried out, the numerical treatment will introduce approximations. Some aspects of these will be considered.

The smallest unit treated by the program is a fuel element. Inside this the flow is assumed to be one-dimensional. In overall calculation a more detailed representation is not possible. Some implications of this approximation will be treated in a later chapter.

In the axial direction of the fuel element both power shape and void profile are discretised. This does not seem to represent a serious problem. In the Dresden reactor the use of 10 axial nodes, that is, a node height of 27 cm is adequate.

In radial direction every fuel element can be treated separately. Even if computing time for the hydraulics is small compared to the computing time for the power shape, it is of interest to know how detailed the hydraulic representation of the core should be.

Generally speaking, fuel elements having the same axial power profile, can be treated as one hydraulic channel. If good knowledge about the power shape exists beforehand, the hydraulics calculation can be performed using only a few channels.

In practice a good representation of the core will demand several calculations, in order to assure its quality. The largest unit, which can be used economically will therefore be the four fuel elements associated with a control rod. For a quarter of the core in the Dresden reactor, this means a reduction from 114 channels, if all fuel elements were treated separately, to 30 channels.

Two calculations have been carried out by means of SYNTRONVOID to check the order of approximation in this.

The same core configuration as in the preceding chapter is used. The control rod setting, which is only changed for channel 17 and channel 25, is shown in fig. 3.2a.

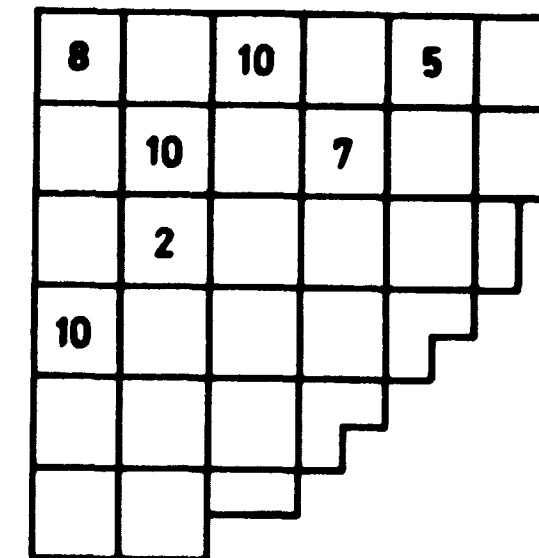


Fig. 3.2a. Dresden 1, quarter core. Control rod setting for test of the influence of the number of hydraulic channels.



In both calculations performed during this investigation, the fine mesh structure was identical. Only the coarse meshes were changed.

The coarse mesh structure for the first calculation is the one of fig. 3.2a. Each of the coarse meshes are associated with one hydraulic channel.

In fig. 3.2b is shown the axial power shape of two of the four fuel elements comprising channel 17. The two elements were those having the highest and lowest power of the four. In fig. 3.2c the average power shape of the four elements is shown. It is the total power of the four elements which is supplied to channel 17 for the hydraulics calculations and it is the average void content of the elements and the total power which determine the cross sections in the coarse mesh associated channel 17.

In the second calculation each of the fuel elements has been represented separately by hydraulic channels. The channels are as shown in fig. 3.2d.

The axial power shapes for the same elements as before are again found in fig. 3.2b. The average power is plotted in fig. 3.2c.

Channel 17 has been chosen since it should have a rather skew flux because of the two neighbouring control rods. As it should be expected the difference in channel power is greatest for the case where only one hydraulic channel is used. In this case all elements have the same cross sections, and the power flattening, because of the channel, with the highest power also having the highest void content, does not exist.

However, the difference between the two cases is only in the order of 3% and it seems to be reasonable in this case to treat four fuel elements as one coolant channel.

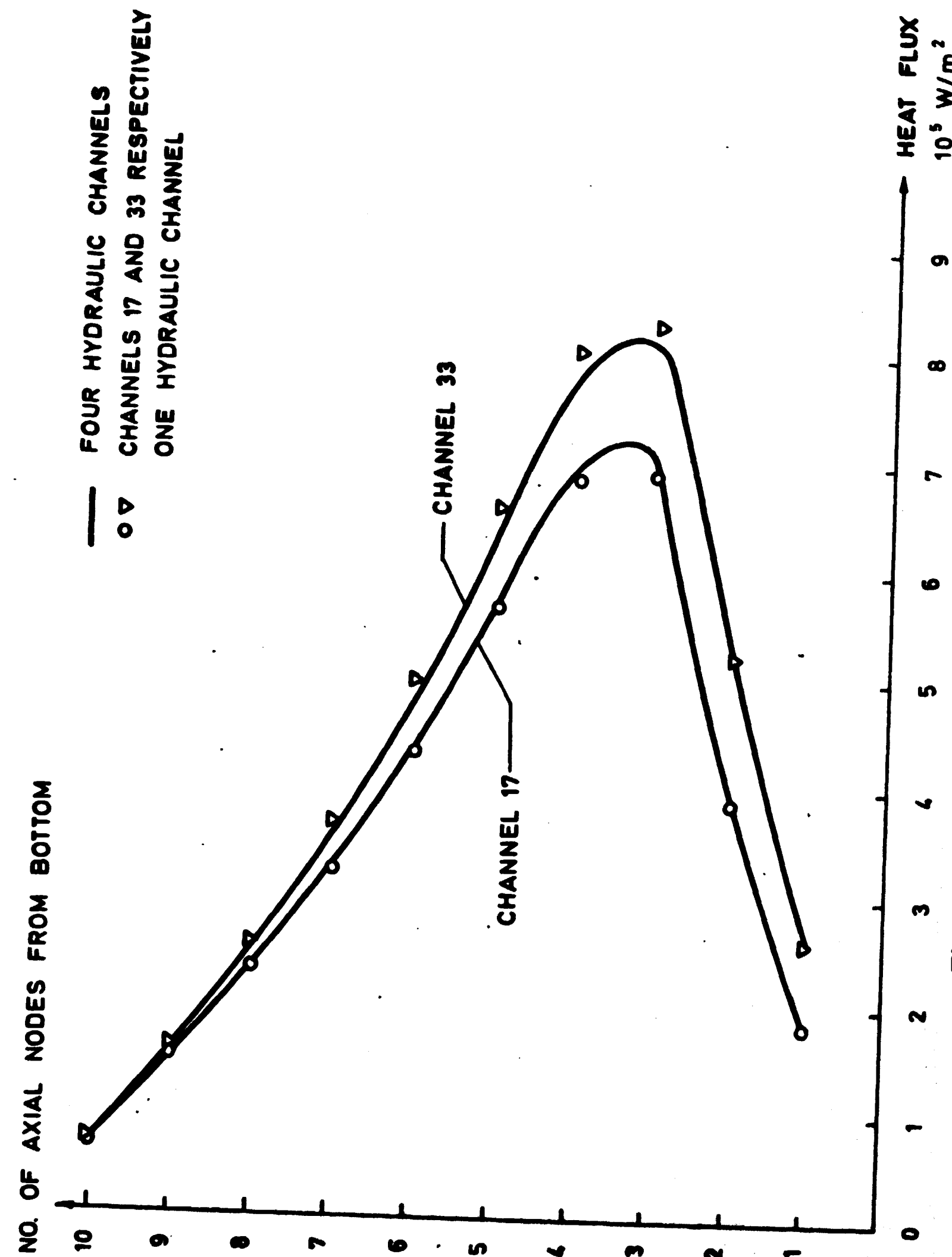


Fig. 3.2b. Axial power shapes for channels 17 and 33.

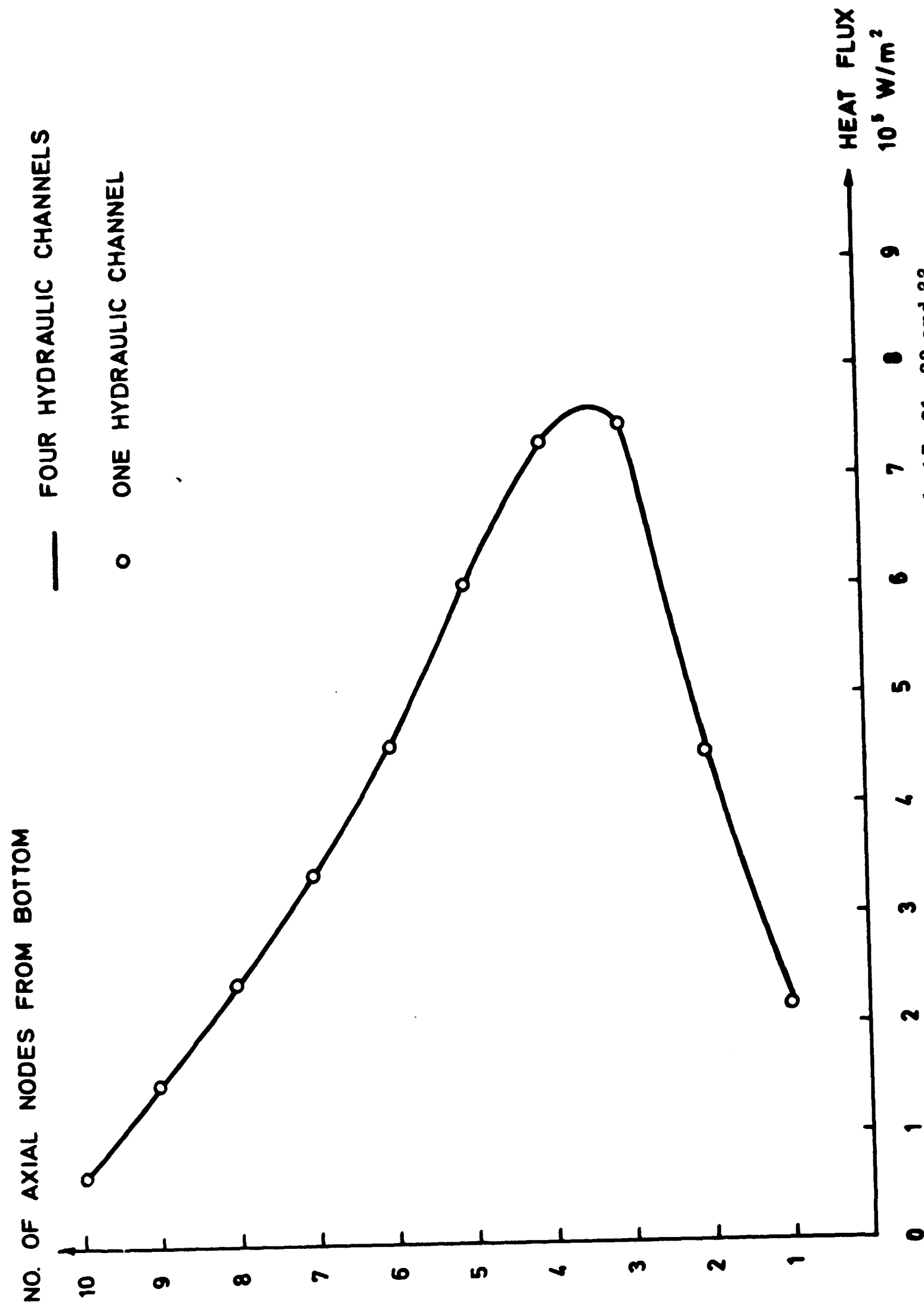


Fig. 3.2c. Average power shape channels 17, 31, 32 and 33.

1	2	5	6	7	8
3	4	13	14	15	16
9	17	31	21	22	23
	32	33			24
10	18	25	26	27	
11	19	28	29		
12	20	30			

Fig. 3.2d. Dresden 1, quarter core. Channel numbering for test of the influence of the number of hydraulic channels.

### 3.3. Concluding Remarks on the Test Calculation for the Hydraulics

The above calculations have all been carried out using data for the Dresden 1 reactor. This, of course, means some lack of generality of the conclusions. Yet it is believed that the conclusions concerning the validity of the physical models for the hydraulics are of general validity, while the conclusions concerning the degree of detail to which a reactor core should be described is dependent of the geometry in hand.

### 3.4. The Flux Synthesis Method

The power distribution in the BWR-simulator is found by means of the flux synthesis method. This method is based on an expansion of the flux shape in so-called trial functions. The flux is given by

$$\phi^g(x, y, z) = \sum_{k=1}^N Z_k^g(z) T_k^g(x, y) \quad (26)$$

where

$\phi^g(x, y, z)$  is the flux group  $g$

$Z_k^g(z)$  is mixing function number  $k$  group  $g$

$T_k^g(x, y)$  is trial function number  $k$  group  $g$

$N$  is the number of trial functions group  $g$

(for a detailed description see ref. 1).

The  $T_k^g(x, y)$ 's are assumed known and (26) is inserted into the diffusion equation. This is then multiplied by some weight functions  $w_k^g(x, y)$  and the  $x, y$  dependence is eliminated by integration over  $x$  and  $y$ . A set of equations for the  $Z_k^g(z)$ 's is thus found.

A condition for this procedure to give reasonable results is that (26) is valid. In case of total separability of the flux shape in axial and radial directions, (26) is evidently valid since the flux is given by

$$\phi^g(x, y, z) = Z^g(z) G^g(x, y) \quad (27)$$

which is identical to (26) for  $N = 1$ .

If, on the other hand, the flux is not separable, one could hope to find a set of trial functions which are complete, or at least will be able to describe the actual flux approximately.

If the problem of finding the flux has been discretised, a set of trial functions, which can describe any flux shape, can be found. These are functions which have the value 1 in a single mesh point and zero elsewhere. The number of trial functions equals the number of mesh points in the  $x$ - $y$ -direction.

The trial functions in SYNTRONVOID and ELGYFO are normally selected to be solutions to two-dimensional difference equations for characteristic horizontal planes.

If the configuration in hand is complicated, there might be several characteristic planes, and this demands several trial functions. As was pointed out in ref. 6 it is necessary to keep the number of trial functions low in order to obtain reasonable computing times. The essential problem of flux synthesis is, if at all possible, to select the proper trial functions.

For a BWR the problem of using flux synthesis is complicated.

Firstly the void content makes the possibility of representing the flux by (26) questionable. It was explained at the beginning of this report that a perturbation of the power by a control rod in the bottom of a fuel element will influence the power of the whole fuel element because of the void. In this manner every horizontal plane will be unique, although the change in cross sections because of voids is not as abrupt as f. ex. at the top of a control rod.

In order to account correctly for the voids, the trial functions used in SYNTRONVOID and ELGYFO are recalculated in each power void iteration. The trial functions for the final power calculation will thus have the correct void content.

Secondly, the fact that the flux distribution for a BWR is found by several iterations between power calculation and hydraulic calculations makes it even more important to keep the number of trial functions low than in situations where only one power calculation is needed.

At the same time it should be remembered that the flux synthesis solution represents an approximation to the difference equation solution of the diffusion equation. A rather fine mesh structure is therefore required.

For the present computer facility (a Burroughs B 6700) this limits the number of trial functions for practical use to 3 or 4.

The problem has already been investigated in ref. 2, ref. 6 and ref. 7. Some additional calculations will be presented in the following.

### 3.5. Examples of Flux Synthesis Calculations for a BWR Geometry

For these calculations a quarter of the Dresden 1 reactor core was again chosen as an example. The core configuration and data were the same as before. All calculations are performed in two energy groups. The actual control rod pattern is shown in fig. 3.5a. As in section 3.1 the numbers indicate the number of nodes, counted from the bottom, the control rods are inserted. Again a fully inserted rod is inserted 10 nodes.

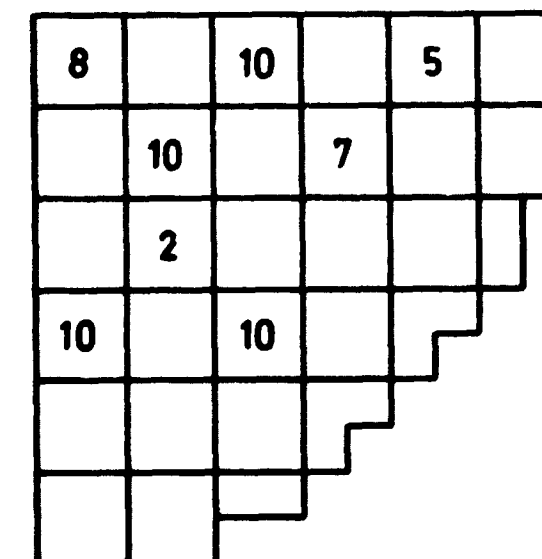


Fig. 3.5a. Control rod setting for test of the flux synthesis method.

The horizontal coarse mesh planes are also numbered from the bottom from 1 to 10. The axial reflector planes in top and bottom are not numbered. The numbering of the hydraulic channels is that of fig. 3.1a. The control rods will be referred to by the number of the hydraulic channel to which it belongs.

In the first calculation two trial functions have been used. These were taken from horizontal planes 1 and 10. The axial power shape in channel 17 is shown in fig. 3.5b.

The next calculation uses three trial functions. These were 1, 3 and 10. The power shape of channel 17 is again plotted in fig. 3.5b.

NO. OF AXIAL NODES FROM BOTTOM

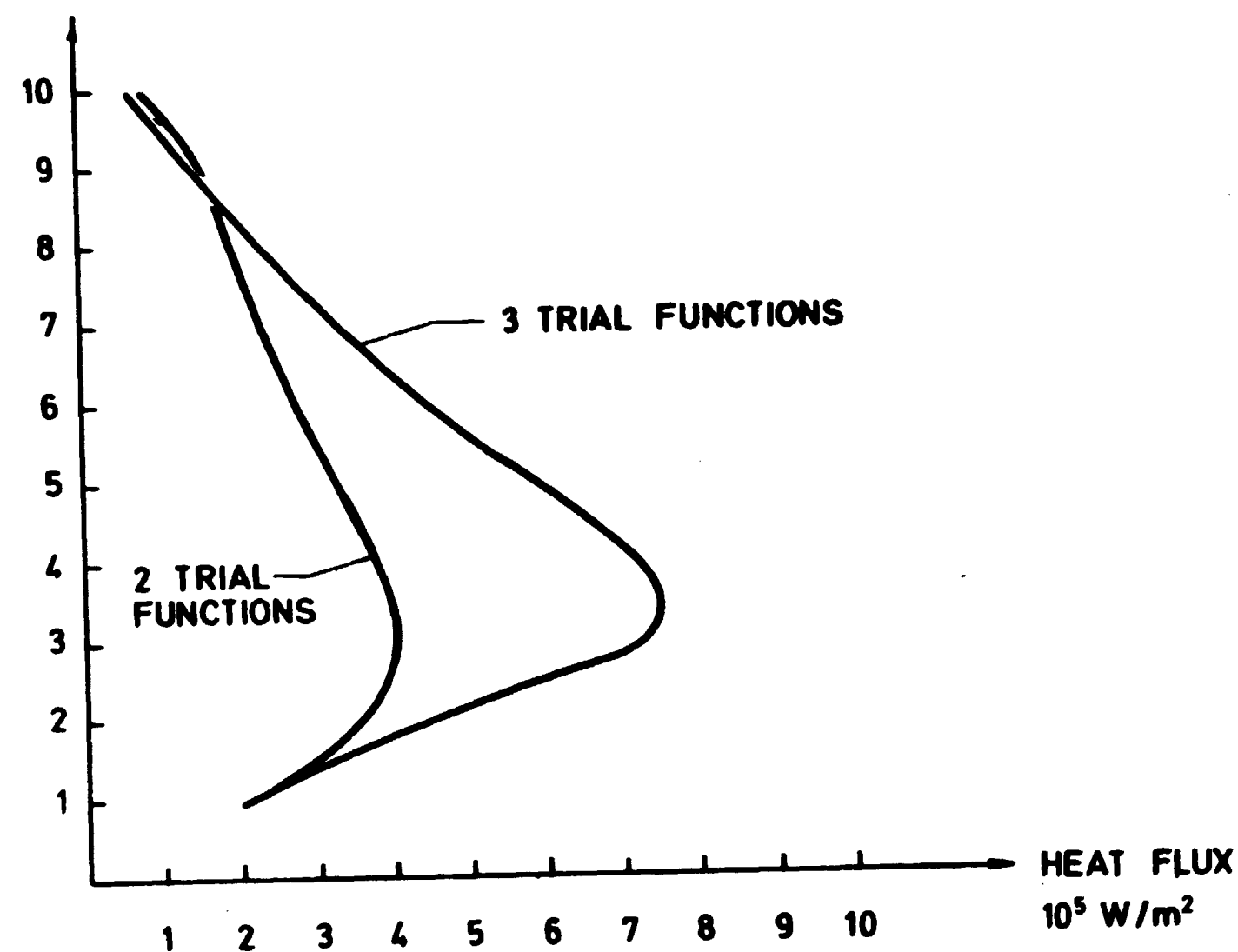


Fig. 3.5b. Power shape channel 17 calculated by flux synthesis.

The change in power shape is very great between the two calculations, and they illustrate the importance of using trial functions enough.

For the following calculations the control rod setting was that of fig. 3.5c. Control rod no. 17 has been inserted 3 more nodes.

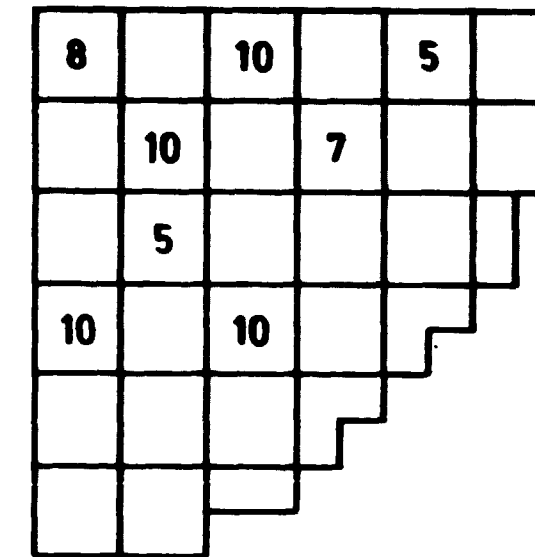


Fig. 3.5c. Control rod setting for test of the flux synthesis method.

In the first calculation three trial functions were used. In analogy with the above they were taken from horizontal planes 1, 6 and 10. In this calculation, as above, each fuel element was represented by four meshes, that is each of the coarse meshes shown in fig. 3.5c was subdivided into sixteen fine meshes.

The axial power shapes from channel 16 and channel 17 are shown in fig. 3.5d and fig. 3.5e.

In the next calculation for the same configuration, four trial functions were used. These were the same as above, and in addition one was taken from horizontal plane no. 8. The power shapes are found in fig. 3.5d and fig. 3.5e.

In the last calculation the upper flux peak in channel 17 is somewhat bigger. This is an effect of the voids, since the only difference in the trial functions from planes no. 8 and no. 10 is the void content.

The following calculation uses the original three trial functions, but the number of fine meshes in the x and y directions was doubled. Each fuel box is now represented by 16 fine meshes. In all cases the number of axial meshes were the same. As before the power shapes from channels 16 and 17 are shown in fig. 3.5d and fig. 3.5e.

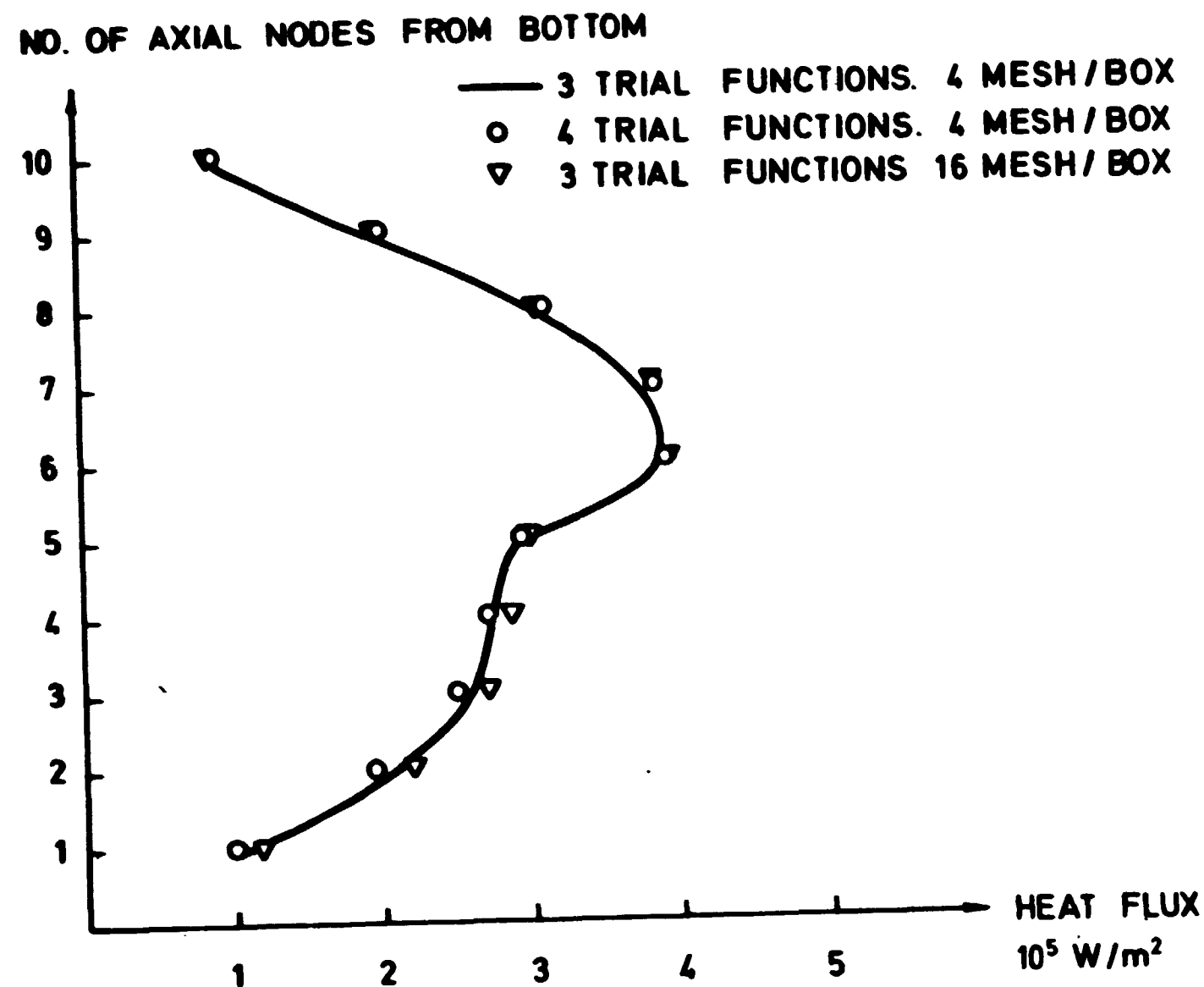


Fig. 3.5d. Power shape channel 16 calculated by flux synthesis.

The axial power shape is quite close to the one found by use of four trial functions. A possible explanation of this is that the finer mesh structure yields a better representation of the flux shape in the trial functions. The flux peaks will be sharper than where fewer meshes are used. When the three-dimensional flux shape is synthesized the flux peaks, which are above control rods 1 and 14, will demand a rather great weight of the trial function from horizontal plane no. 10. This trial function has a high void content in channel 17 and thus a low flux. The flux peaks above control rods 1 and 14 will be in horizontal planes 8 and 9 and a great weight on the trial function from plane no. 10 will flatten the flux peak above control rod no. 17. However, the steeper the flux peaks in the trial functions, the lesser the influence will be on nearby points.

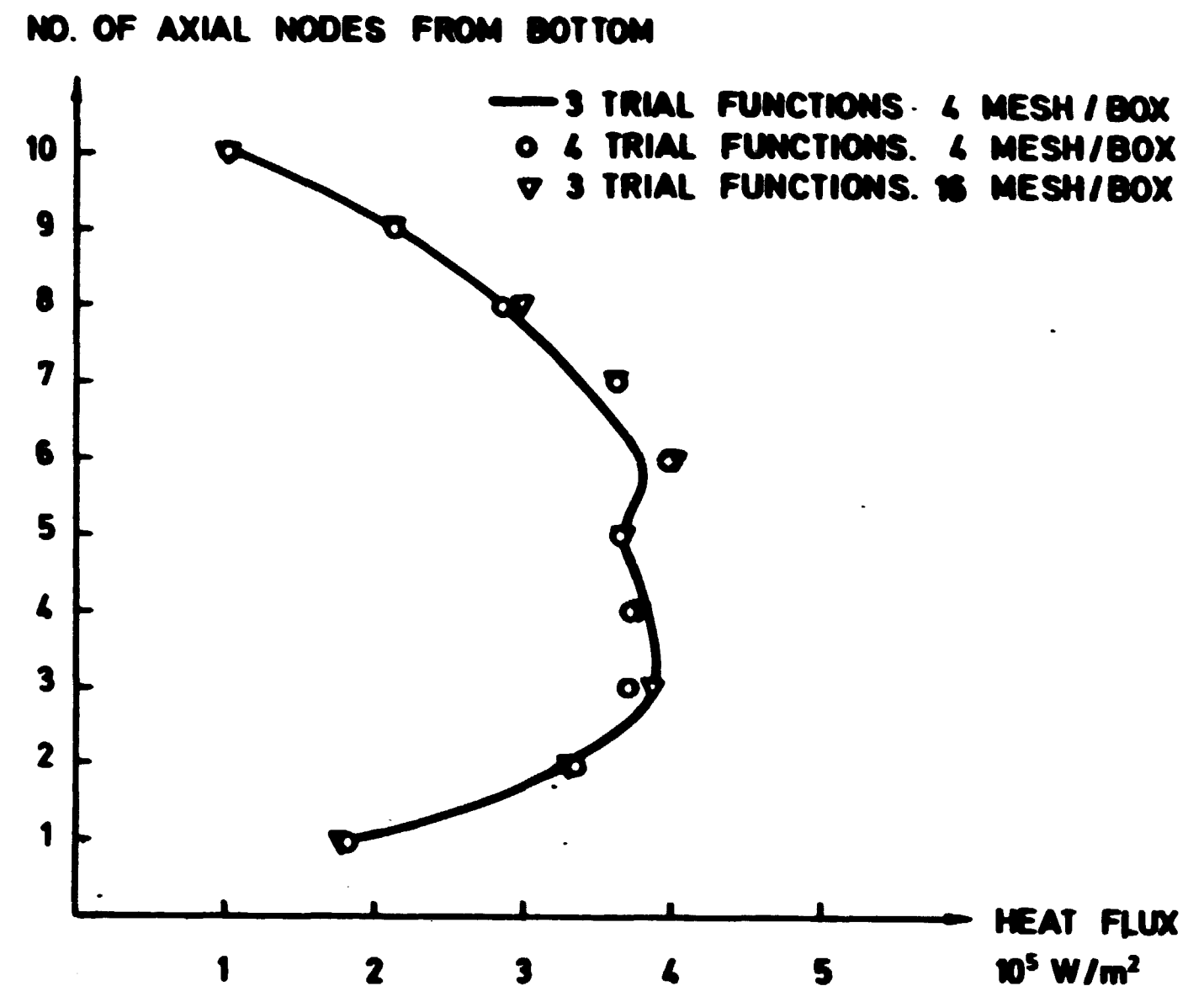


Fig. 3.5e. Power shape channel 17 calculated by flux synthesis.

This explanation is quite unmathematical, but considerations of this kind are the only possible ones when trial functions are selected.

The calculations performed indicate that if an axial flux shape is to be calculated, at least three trial functions are needed if a partially inserted control rod is present. These trial functions might be selected to be flux solutions for horizontal planes in the top and bottom of the core, and the third just above the control rod. If the control rod configuration is complicated, more than three functions might be used.

It has also been illustrated that refining the radial mesh structure will improve the results.

Finally it should be remarked that a set of trial functions selected for finding the flux shape in one channel might be useless for another channel.

The radial flux shape shows the same trends. In fig. 3.5f the power is shown from the last three calculations. To these three a calculation for the same control rod configuration has been added using only two trial functions from horizontal planes 1 and 10. The numbers indicate the average power densities for the channels. The radial reflector is in all cases represented by a Y-matrix<sup>8)</sup> which has been shown in some cases to improve the accuracy of the flux when few meshes are used<sup>7)</sup>. The  $k_{eff}$  for the four calculations are shown in table 3.5a.

77.1	93.0	68.8	113.8	115.7	89.2
69.4	94.0	69.7	118.1	116.5	88.2
78.4	91.7	69.5	113.0	117.1	95.0
95.5	95.7	65.7	101.5	91.8	78.7
116.1	74.0	105.8	88.8	117.0	81.1
116.6	71.4	111.1	101.3	119.8	81.2
115.1	75.4	104.6	91.4	117.0	83.4
118.0	72.2	102.9	98.0	105.7	74.5
123.2	96.1	119.5	124.7	107.9	71.8
122.3	95.3	121.1	127.8	108.8	72.0
121.8	98.3	117.9	122.7	105.8	71.9
119.9	87.4	114.4	121.0	100.8	71.8
84.7	119.7	81.3	103.0	79.4	
81.9	120.7	80.0	102.3	79.6	
86.3	118.1	81.7	98.6	75.3	
86.5	120.0	79.5	98.3	77.5	
137.6	133.0	100.1	71.6		
133.4	130.6	97.3	70.4		
137.3	131.4	96.6	66.6		
151.4	142.5	103.2	72.7		
104.8	89.5	70.9			
101.6	86.9	68.5			
111.7	92.6	70.7			
129.0	106.1	82.4			

1. FIGURE: 3 TRIAL FUNC. 4 MESH/BOX
2. FIGURE: 4 TRIAL FUNC. 4 MESH/BOX
3. FIGURE: 3 TRIAL FUNC. 16 MESH/BOX
4. FIGURE: 2 TRIAL FUNC. 4 MESH/BOX

Fig. 3.5f. Radial power density distribution calculated by flux synthesis.

Table 3.5a

		$k_{eff}$
3 trial func.	4 mesh/box	1.00441
4 trial func.	4 mesh/box	1.00601
3 trial func.	16 mesh/box	1.00118
2 trial func.	4 mesh/box	1.00023

The main conclusion is that the use of only two trial functions does not seem to be sufficient, even if the deviations from flux distributions found by better representations are not as big as for the axial flux shape.

### 3.6. Comparison of Flux Synthesis to Difference Equation Technique

The comparisons carried out until now have all been within the synthesis model itself. This is not sufficient to establish the validity of the method.

A comparison between the synthesis calculation and a difference equation method has been carried out. As test example the above configuration was used. Since no direct coupling to hydraulics is possible for the difference equation program, the cross sections used were obtained as follows.

Just before the final power calculation during the power void iterations in SYNTRONVOID the cross sections, coarse mesh by coarse mesh, for the whole core were punched on cards. These were fed into the DC4 program<sup>9)</sup>. The SYNTRONVOID calculation spoken of was the one using the three trial functions from horizontal planes 1, 6 and 10 and 4 fine meshes per fuel box. In the difference equation calculation the radial reflector was represented by the same Y-matrix as before.

Again the axial power shapes from channels 16 and 17 have been plotted (fig. 3.6a and fig. 3.6b). These shapes have been compared to the SYNTRONVOID calculations from which the cross sections originate. In fig. 3.6c the radial power distributions are found.

As it could be suspected, the axial power shapes calculated by the synthesis method do not agree very well with the shapes computed by difference equation technique. That degree of separability, which is a demand for the synthesis to work properly with few trial functions, is not present in

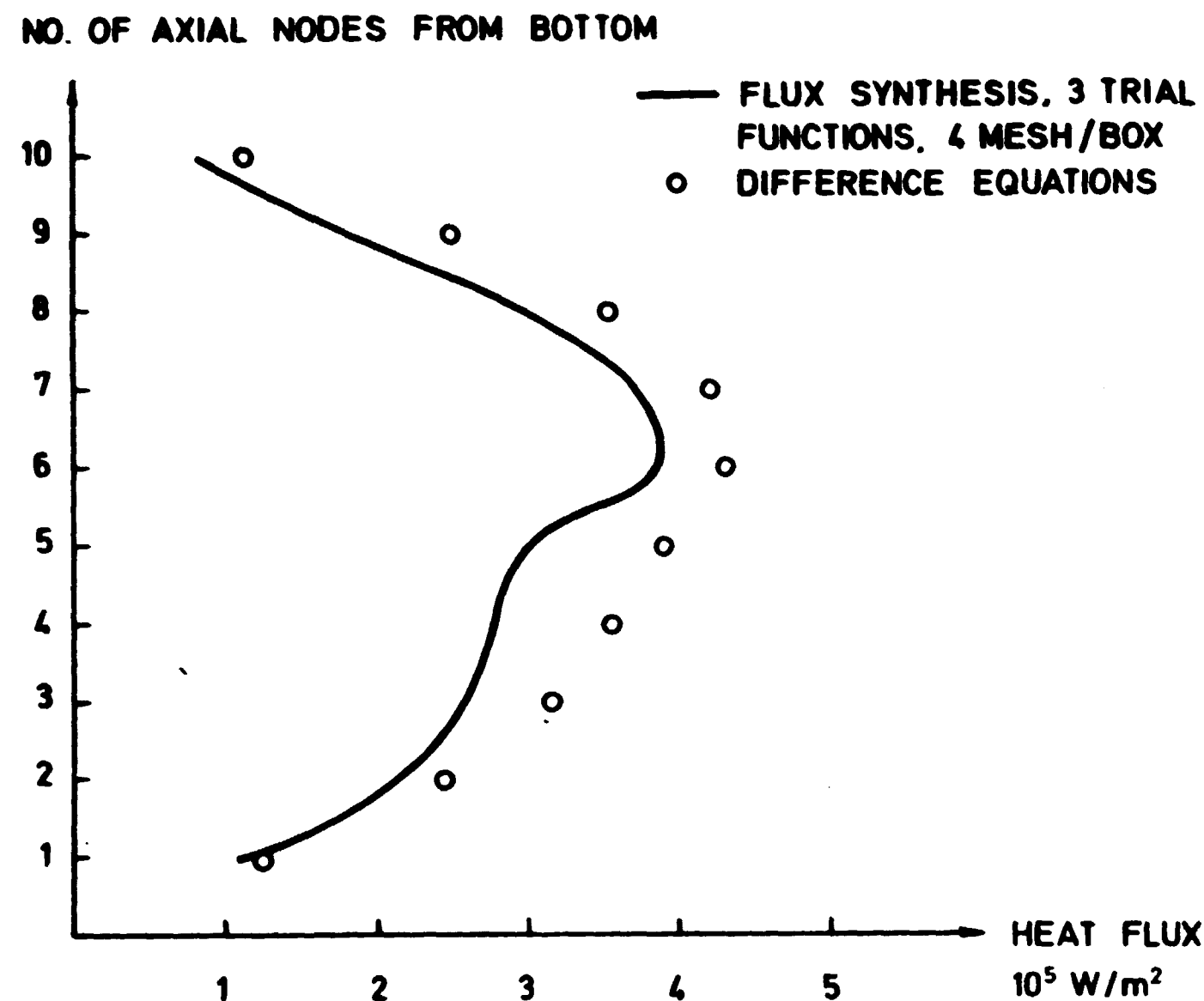


Fig. 3.6a. Power shape channel 16. Comparison between flux synthesis and difference equation technique.

the actual flux shape. The assumption that (26) was able to represent the flux, impose some separability on the problem. In this manner the flux peak above control rod 17 is levelled out, and the flux in the lower parts of channel 16 is lowered.

The agreement in radial power distribution is not very good, but different factors which influence the difference equation calculation should be considered.

At first the DC4 program uses the mesh point when the diffusion equation is discretized, whereas SYNTRONVOID uses average fluxes. The DC4 calculation is in  $39 \times 39 \times 36$  meshes which is the maximum obtainable on the present computer installation. The meshes were situated to yield the best possible representation of the actual flux shape. Yet, the fluxes are estimated only to be within 13% of the correct calculation.

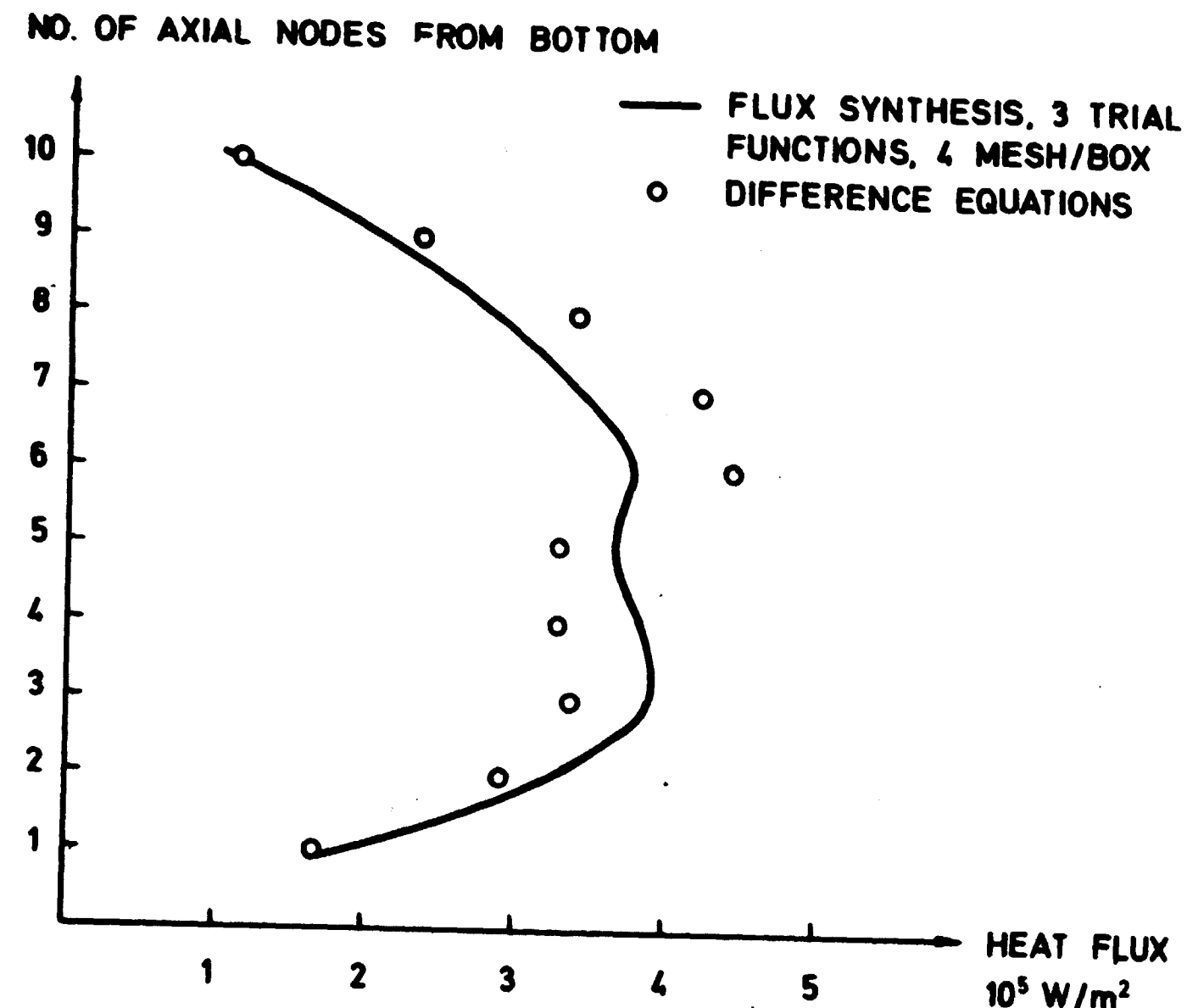


Fig. 3.6b. Power shape channel 17. Comparison between flux synthesis and difference equation technique.

Any conclusion concerning the radial power is thus difficult to draw, but the results for the axial shape are not altered. Even if a 13% uncertainty is taken into account the power shapes found by the difference equation method seem much more probable.

77.1	93.0	68.8	113.8	115.7	89.2
72.9	96.6	86.7	134.2	129.8	108.4
116.1	74.0	105.8	88.8	117.0	81.1
107.2	83.4	118.3	120.3	139.8	97.8
123.2	96.1	119.5	124.7	107.9	71.8
109.3	97.5	123.6	136.8	123.7	81.2
84.7	119.7	81.3	103.0	79.4	
74.9	98.6	82.3	103.2	80.6	
137.6	133.0	100.1	71.6		
98.4	99.4	82.3	61.6		
104.8	89.5	70.9			
80.0	68.6	55.6			

1. FIGURE: FLUX SYNTHESIS
2. FIGURE: DIFFERENCE EQUATIONS

Fig. 3.6c. Radial power density distribution. Comparison between flux synthesis and difference equation technique.

### 3.7. Comparison with Nodal Theory

As a last calculation a nodal theory calculation has been carried out by means of the nodal theory part of the ANDYCAP<sup>10)</sup> program.

The cross sections were the same as for the DC4 calculation. In ANDYCAP the reflectors have to be represented by an albedo. This albedo was roughly fitted to yield a radial power distribution equal to the one found by DC4. The internal coupling coefficients were taken over from a calculation for another BWR. Each fuel element was represented by one node in radial direction and ten nodes in axial direction.

In fig. 3.7a and fig. 3.7b the same axial power shapes as before are found together with the DC4 solutions. The radial power is in fig. 3.7c.

The radial power from the nodal theory calculation is in fairly good agreement with the DC4 calculation. This was of course to expect since the albedos have been adjusted to yield this. By a better adjustment of the coupling coefficients an even better agreement is expected.

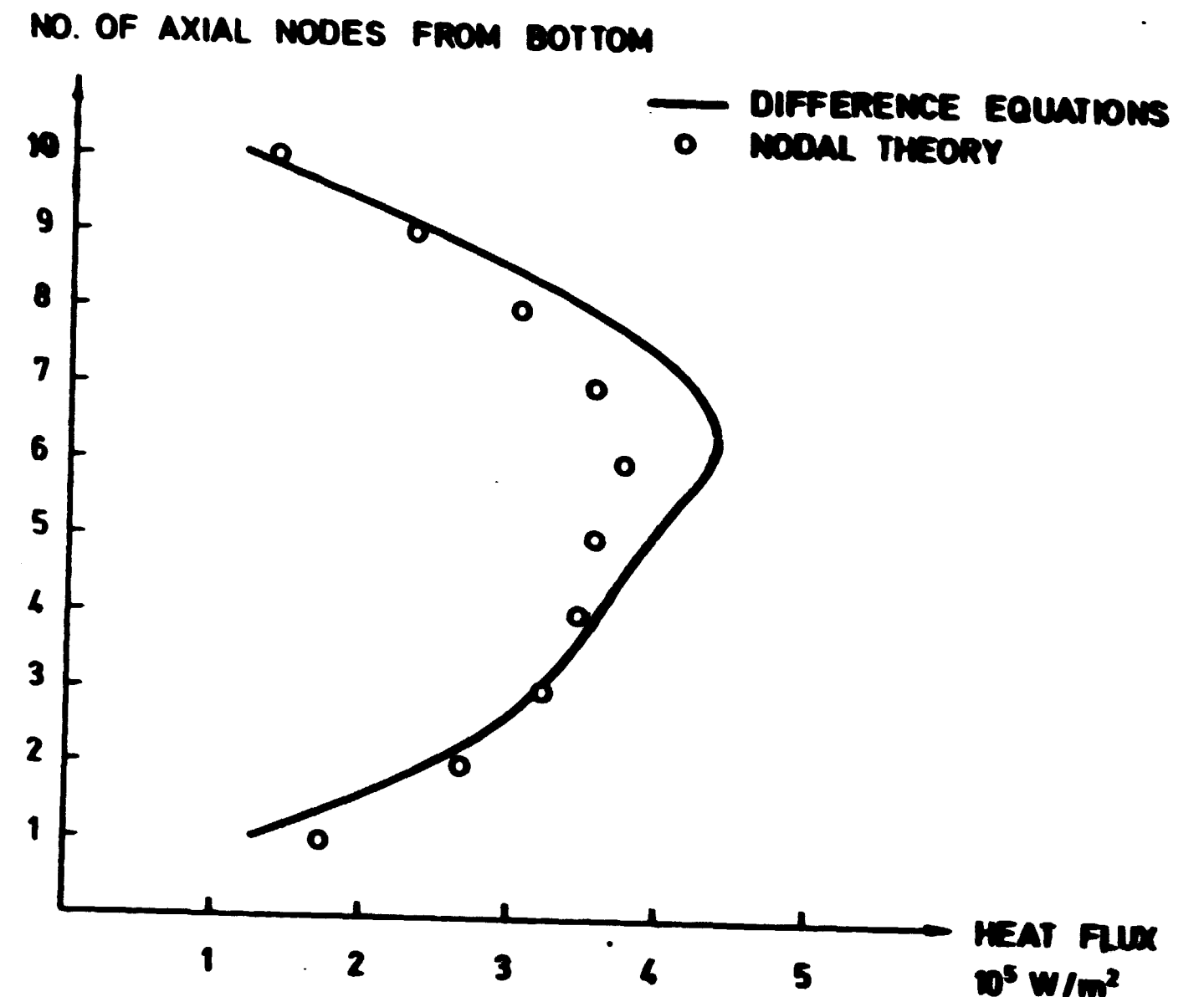


Fig. 3.7a. Power shape channel 16. Comparison between difference equations technique and nodal theory.

What is important to remark is that the axial power shapes seem to be more in agreement with what is expected from the DC4 calculation than the synthesis results.



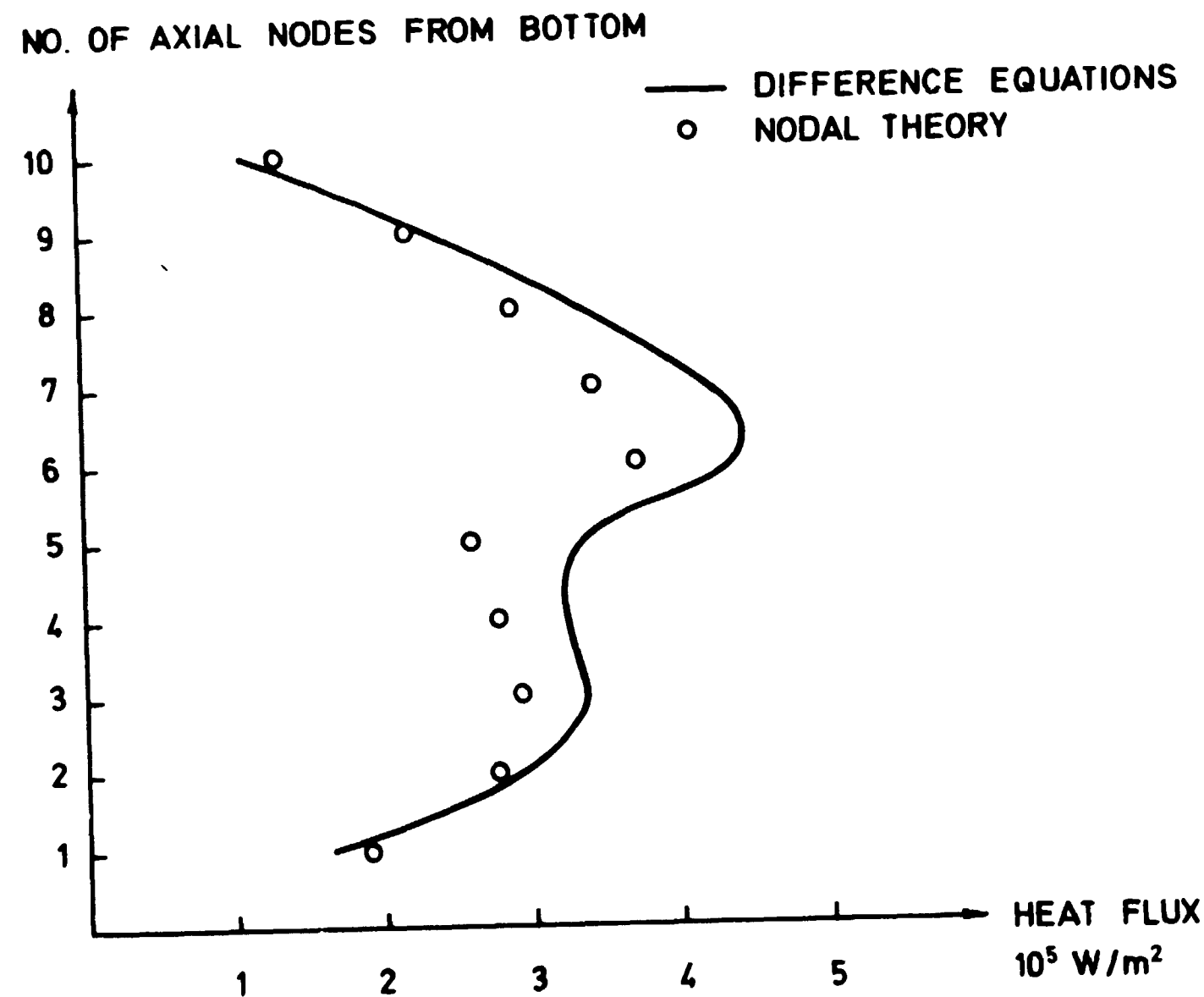


Fig. 3.7b. Power shape channel 17. Comparison between difference equation technique and nodal theory.

72.9 69.5	96.6 87.0	86.7 83.3	134.2 125.3	129.8 122.8	108.4 98.3
107.2 94.5	83.4 78.8	118.3 113.0	120.3 124.3	139.8 142.5	97.8 96.5
109.3 96.3	97.5 93.3	123.6 122.3	136.8 145.3	123.7 144.5	81.2 106.5
74.9 70.5	98.6 93.8	82.3 90.3	103.2 123.3	80.6 108.7	
98.4 86.0	99.4 93.8	82.3 93.5	61.6 84.0		
80.0 67.3	68.6 63.3	55.6 68.5			

1. FIGURE: DIFFERENCE EQUATIONS  
2. FIGURE: NODAL THEORY

Fig. 3.7c. Radial power density distribution. Comparison between difference equation technique and nodal theory.

### 3.8. Concluding Remarks on the Synthesis Method

The trial functions for the described calculations are not the only possible, but seem to be the most reasonable. It was seen that the synthesis method might completely fail to calculate certain axial flux shapes. Addition of specially constructed trial functions might improve the results. If one is interested in f. ex. the flux peak above a control rod, a trial function containing a flux peak at the situation of the control rod and zero elsewhere may have this effect.

Firstly, however, this will increase the computer time spent, since the original three or more trial functions are still needed to give a good determination of the power distribution. In order to give some impression of the needed computer time, the above described calculation with nodal theory uses about the same amount of time as the synthesis calculation with three trial functions and 4 meshes per fuel box.

Secondly some test calculation will be needed to confirm the possible improvement of an extra trial function. Another important result of the above synthesis calculations is namely that addition of an extra trial function or refining the mesh size do not alter the results considerably, even if the obtained results deviate from the correct answer. One might therefore stop to improve the calculations too early.

#### 4. SUBCHANNEL CALCULATIONS

Until now the coolant flow in the fuel elements has been considered to be one-dimensional. For overall calculations this is sufficient, also because the nuclear cross sections inside a fuel box will be homogenized.

When a detailed calculation is carried out for a fuel box in order to determine local form factors and burn up, the nonuniform distribution of steam voids might have some effects. The fuel pin having the highest power will also produce the highest void content in its surroundings with a subsequent power flattening. Also change in spectrum and thereby change in burn up behaviour might be caused.

In a BWR it is mainly the water gaps surrounding the fuel box, which create the power peak. When no other steps are taken to flatten the flux, the highest flux peak will be at the corner close to the broadest water gaps. Even if the void content around the corner pin is high, the moderating of the water gaps, which are within half a diffusion length, will be present and tend to decrease the flattening effect of the nonuniform void distribution.

##### 4.1. Effect of Nonuniform Void Distribution on the Power Distribution in a Dresden 1 Fuel Box

A number of calculations have been set up for estimating the order of magnitude of the reduction in radial power form factor in a Dresden 1 fuel box.

This fuel box is not typical for a modern BWR. In modern BWR's different enrichment of the fuel pins and burnable poison is used to lower the form factor. A lower form factor will create a lesser nonuniform void distribution and the flattening effect is thus reduced. In the Dresden 1 fuel box, the radial form factor is as high as 1.31 to 1.35 for a nonuniform void content of 0% and 60% respectively. This should be borne in mind when the results are considered.

The detailed void distribution is calculated by means of the subchannel program SDS<sup>11)</sup>. This program is designed to carry out thermal hydraulic

analysis of BWR fuel elements. The fuel element is radially divided into subchannels as shown in fig. 4.1a. Each subchannel interacts across the gaps between fuel rods with its neighbouring channels. The interactions are both net cross flow and mixing, that is interaction without net transfer of mass. In this manner a three-dimensional analysis is performed.

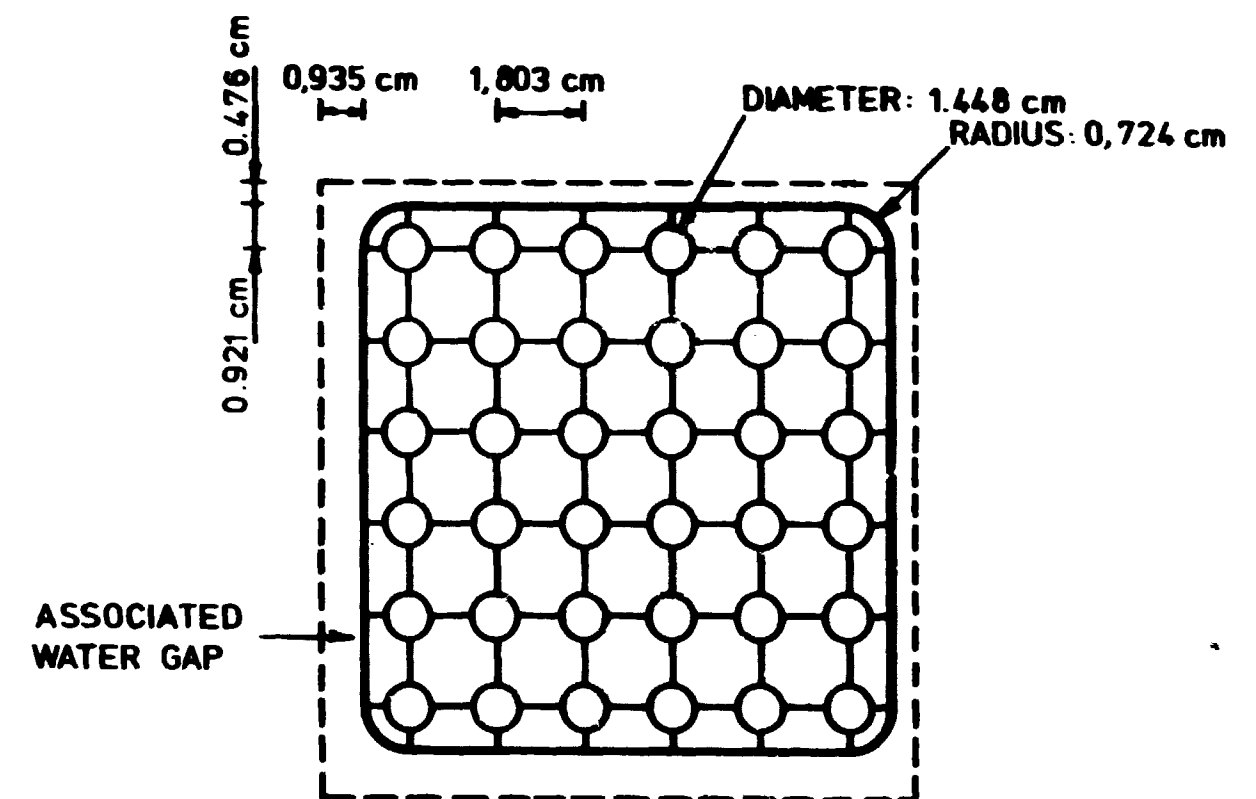


Fig. 4.1a. Horizontal cross section and subchannel division for Dresden 1 fuel element.

As input data for the SDS program should be given, besides geometrical data and material properties of water, a radial power distribution and an axial power distribution.

The relative axial power distribution for the present calculations was taken from an overall calculation for the reactor. The power shape of fig. 3.2c was used.

For the first calculation by SDS, the radial power shape was taken from a CDB<sup>12)</sup> calculation for a Dresden fuel box with no void.

CDB is a fuel box burn up program using a collision probability method for calculating flux in the pin cells and diffusion theory for the flux calculation in the fuel box. In all calculations ten energy groups, of which six

were in the thermal region, were used. In the diffusion calculation five groups were used. In this case two were thermal groups. The cross sections were those used in ref. 2 for hot clean conditions. For the first calculations no burn up calculation is performed. Only the power shape has been determined by CDB.

The calculated detailed void distribution from the horizontal position, at which the axial power peak is situated, is then put into CDB. The moderator density for the pin cells in CDB is calculated as arithmetic mean of the density of the four subchannels adjacent to the fuel pin.

The alternating calculations by CDB and SDS is continued until a converged power shape is obtained.

Fig. 4.1b shows the final radial power distribution and the power distribution found by use of uniform void distribution in CDB. In fig. 4.1c the final void distribution is found.

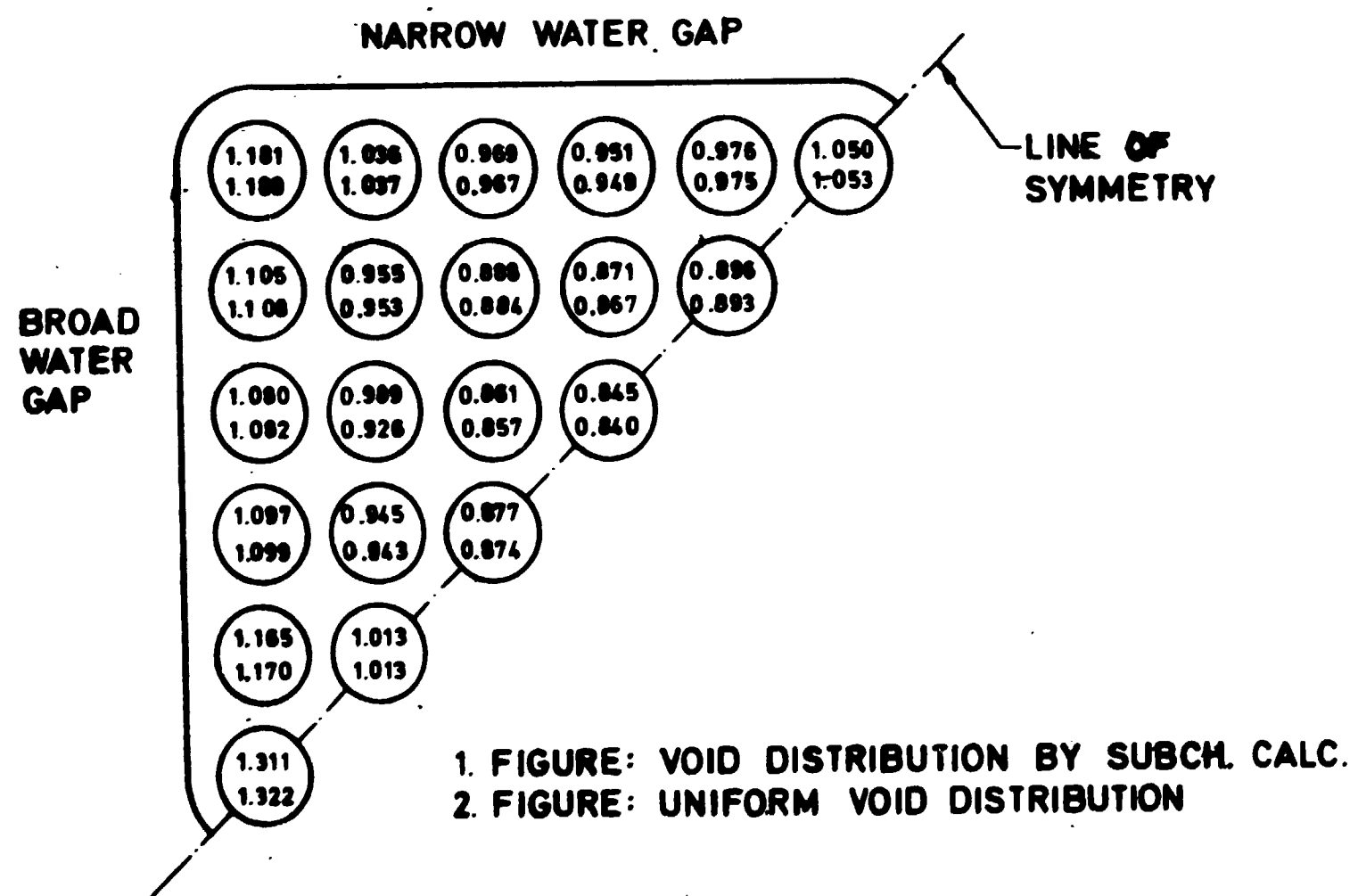


Fig. 4.1b. Relative radial power distribution in Dresden 1 fuel element. Horizontal position at axial power peak.

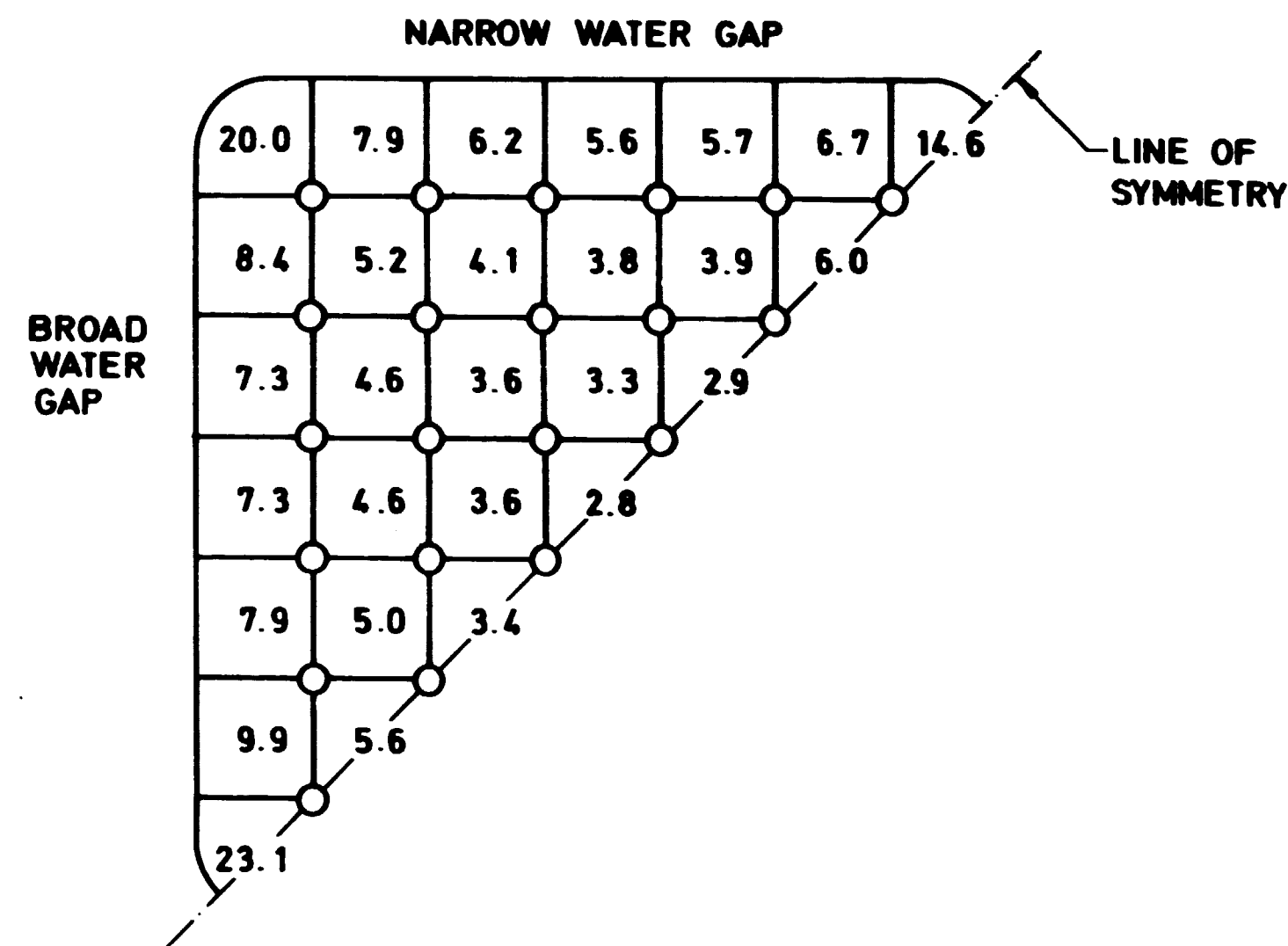


Fig. 4.1c. Radial void distribution (%) in Dresden 1 fuel element. Horizontal position at axial power peak.

The same procedure as above is carried out for the same fuel element, but in this case the radial power distribution in the top is considered.

The results are found in fig. 4.1d and fig. 4.1e.

At the axial flux peak the reduction in power shape is 0.8%. Compared to the normal calculation accuracy this is negligible.

At the top, where the average void content is higher, the flattening is 4.3%. Since those parts of a BWR core where the void content is high also have a low power density, the effects on the total burn up or calculation of margins will be small. At least they do not justify the rather time consuming calculations by a subchannel program.

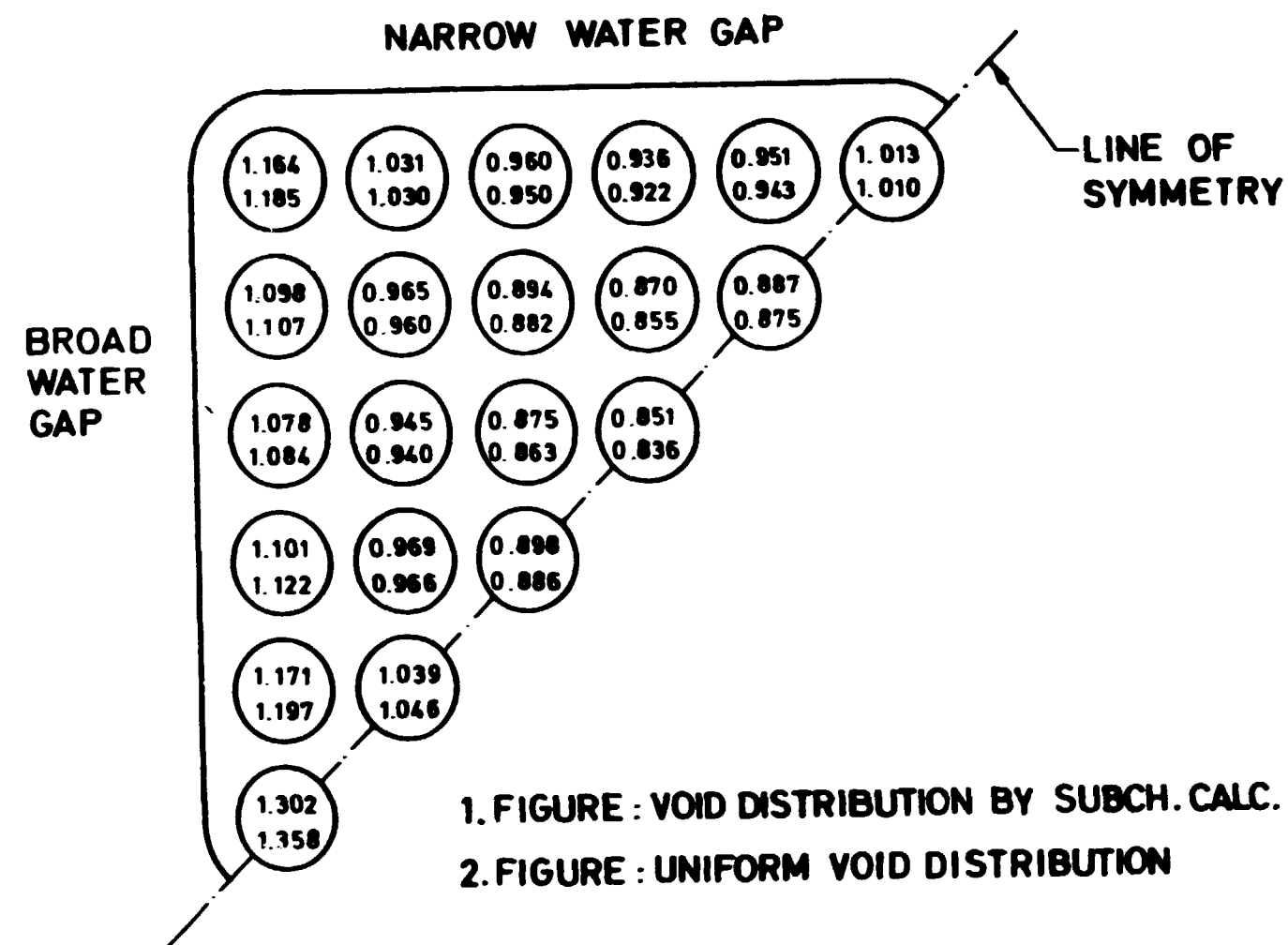


Fig. 4.1d. Relative radial power distribution in Dresden 1 fuel element. Horizontal position at top of element.

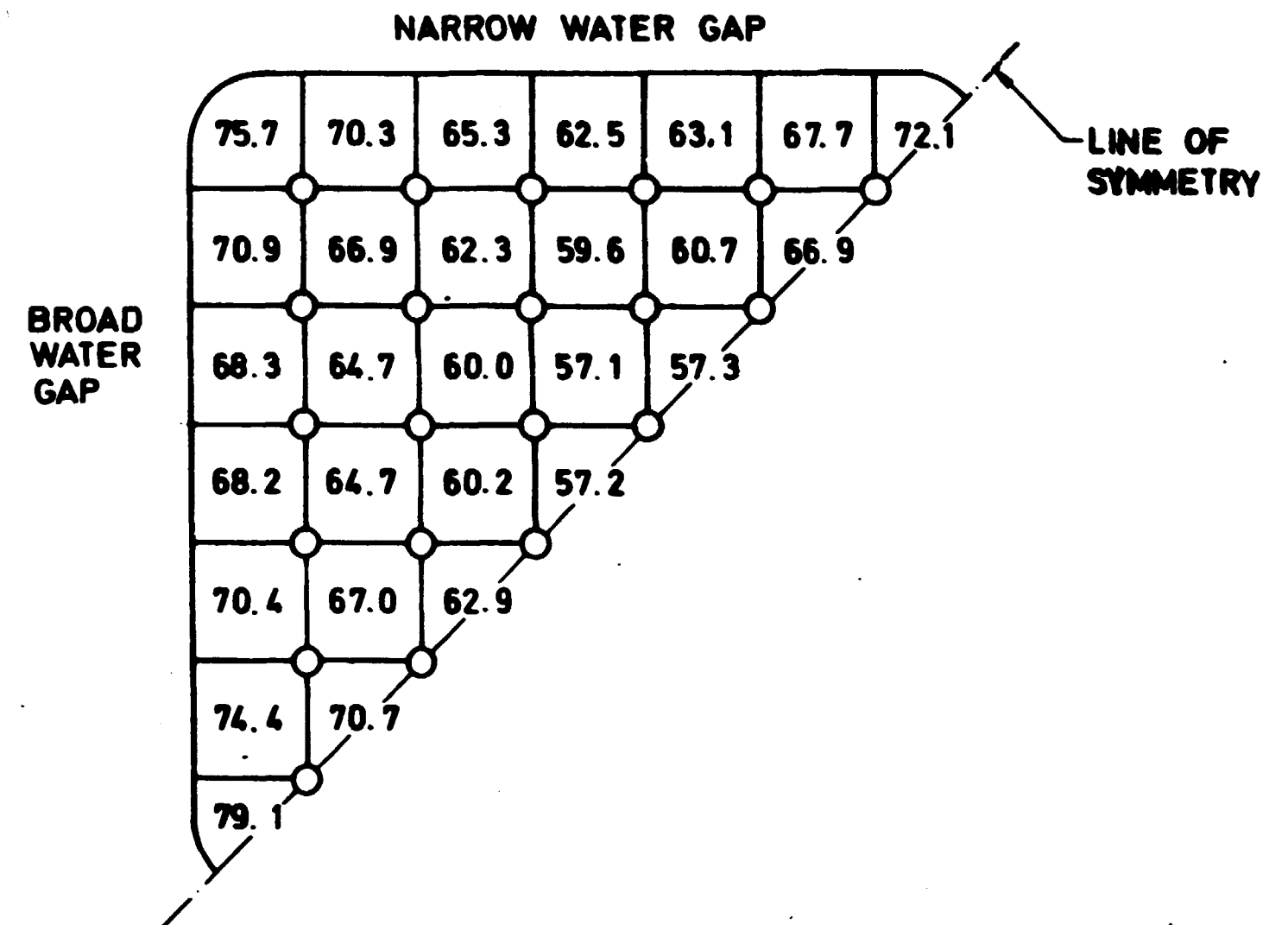


Fig. 4.1e. Relative void distribution (%) in Dresden 1 fuel element. Horizontal position at top of element.

#### 4.2. Spectrum Effects of Inhomogeneous Void Distribution in a Dresden 1 Fuel Box

The spectrum effects of the non-uniform distributed void are even less than the effects on the power distribution.

Both the uniform and non-uniform void distributions from the top of the fuel element where the effect is believed to be greatest, have been used in a burn up calculation in CDB. The difference in spectrum in terms of the ratio of total Pu built up to  $U^{235}$  is not possible to detect.

## 5. BURN OUT CALCULATIONS

The overall power distribution forms the basis for determining several operating margins in a reactor. One of the most important is the burn out margin.

The mechanisms leading to burn out are not well understood or described. Probably several conditions have to co-exist for burn out to occur. Predictions of burn out until now totally rely on experimental fitted correlations. Because the physical phenomena taking place are many and little known, these correlations are tightly connected to the experiment they are correlated to. Extrapolations to situations different from the original one are more dubious than for correlations for heat transfer etc. where the processes taking place are described in some detail.

According to Tong<sup>13,14)</sup> two types of burn out exist.

One is fast burn out, which occurs at low steam quality and high sub-cooling. It occurs at high heat fluxes.

The high heat flux produce a high density of vapour bubbles near the heated wall. The bubbles prevent liquid to reach the wall and the cooling of the wall is reduced and its temperature will rise rapidly.

This type of burn out is dependent on conditions near to the heated surface and of the heat flux. It is thus a local phenomenon.

The second type is slow burn out, or dry out. This occurs at high steam quality. Normally the flow regime is annular when dry out takes place. The heated wall is covered by a liquid film which provides the cooling. If the evaporation is high, the film might break down and burn out will occur.

In this case the heat flux alone at the situation of the burn out is not as important as before, but the integrated power upstream is also important since it determines the steam quality at the situation of the burn out.

It is seen that when the total power of a fuel element is increased, burn out of the second type will appear first at the exit, for uniformly heated fuel elements.

These explanations are very short summaries of what is found in ref. 13 and ref. 14. It should be remarked that in practice there is no sharp boundary between the two forms. However, it is seen that in order to predict burn out margins in a reactor both integral power of the fuel elements and power peaks should be calculated correctly.

### 5.1. Burn Out Correlation for SYNTRONVOID and ELGYFO

In both SYNTRONVOID and ELGYFO a correlation for calculating critical heat flux is incorporated. The correlation calculates for a given point in the fuel element that heat flux which should exist at that point for burn out to occur. Comparing the critical heat flux with the actual heat flux, one is able to estimate how far from burn out conditions the fuel element is. In this connection it is emphasized that burn out is no linear phenomenon. If the actual heat flux is half the critical heat flux, the actual flux might not be raised almost by a factor of two, without burn out to occur. Since the heat flux at a certain point of a reactor cannot be increased without the surroundings also increasing their power, an increase in heat flux is accompanied by an increase in steam quality. The critical heat flux is thus decreased.

The correlation is the Becker correlation<sup>15)</sup> based on the Vanderwater-Isbin model<sup>16)</sup>. The model assumes a flow composed of a liquid film on the heated surface, and outside this a flow of steam and droplets. These phases interact, and when the film dries out, burn out occurs. The correlation is thus designed for predicting burn out in the high quality region, but it has been correlated also to be valid for low qualities.

The data for the correlation are originally obtained from round ducts. For fuel elements it has been fitted by a transformation of the actual steam quality to an equivalent round duct quality. Also the radial power form factor for the fuel element is taken into account. Used for fuel elements, the correlation is believed to predict critical heat flux within  $\pm 25\%$ .

### 5.2. Comparisons between the Becker Correlation and General Electric Design Criterion

In order to demonstrate a burn out calculation the Dresden reactor has been put on 100% overpower and the total coolant flow has been reduced by 30%.

A calculation is carried out including calculations of critical heat fluxes by means of the Becker rod bundle correlation. The channel, in which the heat fluxes are closest to critical heat flux, is sought out. The control rod pattern was that of fig. 3.5a and the channel turned out to be no. 19 (fig. 3.1a). For this channel the mass flow rate was  $565 \text{ kg/sec m}^2$  and the exit steam quality 55%.

The actual heat fluxes and critical heat fluxes along the channel have been plotted versus enthalpy quality (see equa. (4)) in fig. 5.2a. In fig. 5.2a

is also shown the General Electric design criterion<sup>17)</sup>. The GE criterion is not constructed to predict burn out. It is a set of limiting curves of heat flux versus enthalpy quality below which experience has shown that burn out will not occur. The criterion is thus rather conservative. It has the form:

$$\begin{aligned} \varphi/10^6 &= 2.222 + 5.507 \cdot 10^{-4} \cdot G & \text{for } x < x_1 \\ \varphi/10^6 &= 5.151 - 6.277 \cdot 10^{-4} G - 13.146 x & \text{for } x_1 < x < x_2 \\ \varphi/10^6 &= 1.907 - 3.811 \cdot 10^{-4} G - 2.059 x & \text{for } x > x_2 \end{aligned} \quad (28)$$

where

$$x_1 = 0.197 - 7.963 \cdot 10^{-5} G$$

$$x_2 = 0.254 - 1.917 \cdot 10^{-5} G$$

$x$  is the enthalpy quality.

$G$  is the mass velocity in  $\text{kg/sec m}^2$ .

$\varphi$  is the limiting heat flux in  $\text{W/m}^2$ .

HEAT FLUX  
 $10^6 \text{ W/m}^2$

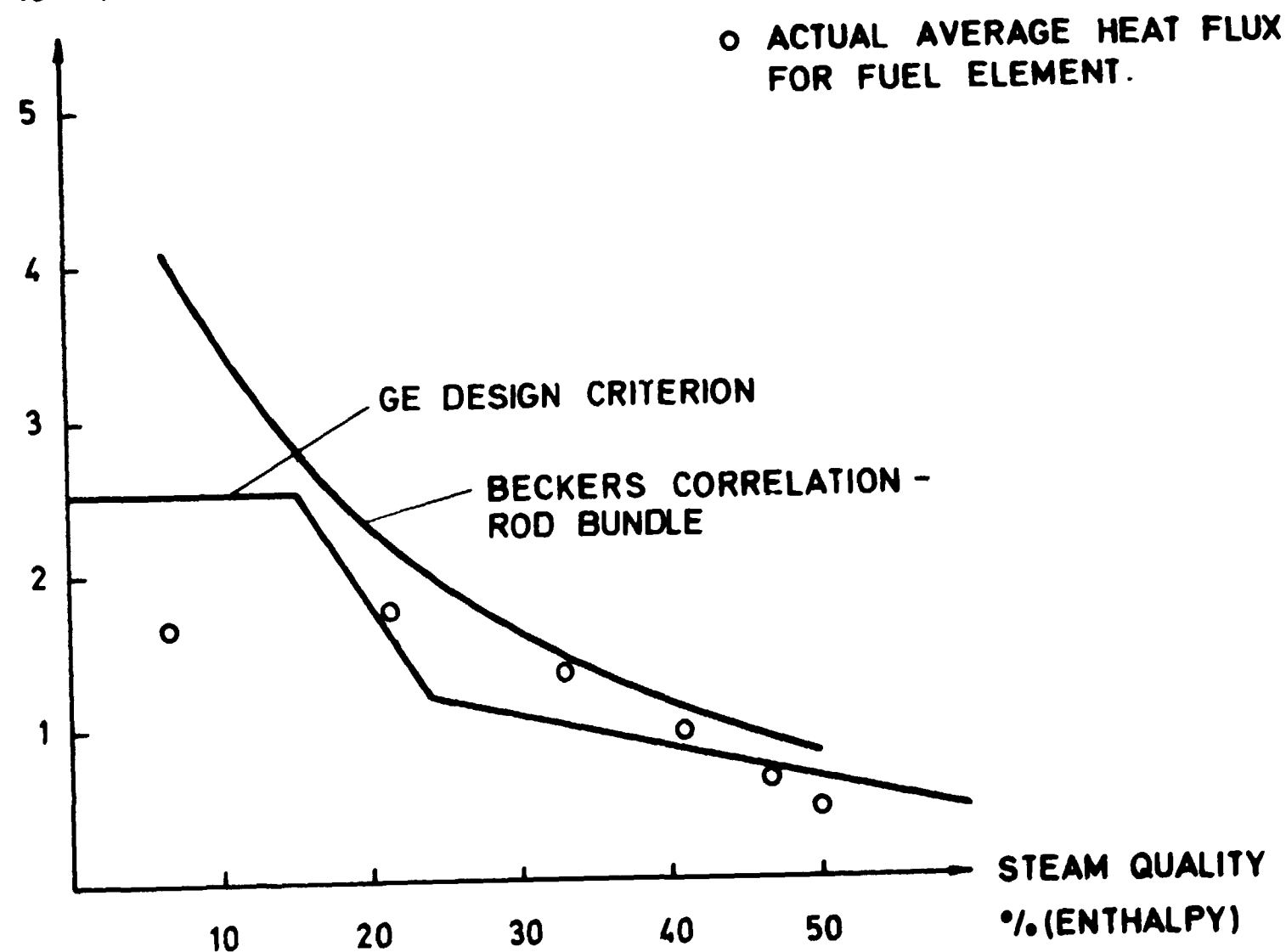


Fig. 5.2a. Burn out prediction in Dresden 1. (Channel 19).

The criterion is valid for  $G$  up to  $8 \cdot 10^3 \text{ kg/sec m}^2$ , hydraulic diameters below 1.5 cm and a pressure of around 69 bars. For other pressures  $\varphi$  is found from

$$\varphi = \varphi_{p=69} + 6381 \cdot (69 - p) \quad (29)$$

As expected the critical heat fluxes predicted by the Becker correlation are above the GE criterion. In the low quality region the Becker correlation predicts a critical heat flux much higher than the GE criterion. However, the transformation of rod bundle qualities to round duct qualities in this region, where the burn out phenomenon is local, has not been fitted correctly. The critical heat fluxes predicted by the Becker correlation for low qualities should therefore be treated with some caution.

### 5.3. Burn Out Calculations by Subchannel Analysis

Considering the results in fig. 4.1e it is seen that the radial distribution of steam in a fuel element is far from being uniform. It seems to be obvious that if the actual steam quality distribution in a fuel element is known, this yields a better background for predicting burn out than using the average value. Evangelisti et al<sup>18)</sup> have shown for certain experiments that if a subchannel calculation is carried out for a fuel element, and the division into subchannels shown in fig. 5.3a is used, Beckers correlation for round ducts used for these subchannels predicts burn out within around 5%.

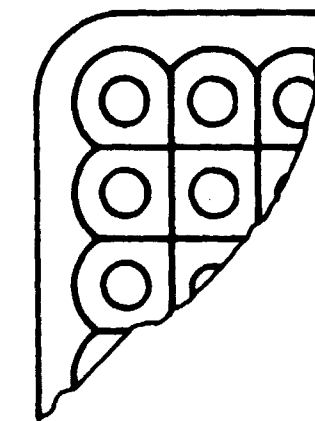


Fig. 5.3a. Subchannel division for calculation of burn out according to Evangelisti et al.

To illustrate the above, a subchannel calculation was carried out for one of the fuel elements in the Dresden reactor (channel 19). The mass flow rate and axial power distribution were obtained from the SYNTRONVOID calculation described in section 5.2. The radial power distribution was taken from a CDB calculation. The radial form factor was 1.3.

The SDS program is not able to treat subchannels as shown in fig. 5.3a. Instead those shown in fig. 4.1a were used. The steam quality and mass flow rates which formed the basis of the burn out calculation were then obtained from the four subchannels surrounding a fuel pin as

$$x = \frac{x_1 w_1 + x_2 w_2 + x_3 w_3 + x_4 w_4}{w_1 + w_2 + w_3 + w_4} \quad (30)$$

$$w = (w_1 + w_2 + w_3 + w_4)/4 \quad (31)$$

where

$x_i$  is the steam quality

$w_i$  is the mass flow rate

The critical heat flux for the corner pin having the highest power was calculated by means of the Becker correlation for round ducts. The critical heat fluxes and actual heat fluxes are plotted versus steam quality (weight %) in fig. 5.3b. At 22.5% there is a weak change of slope on the curve which represents the transition between correlations for the low and the high quality regions.

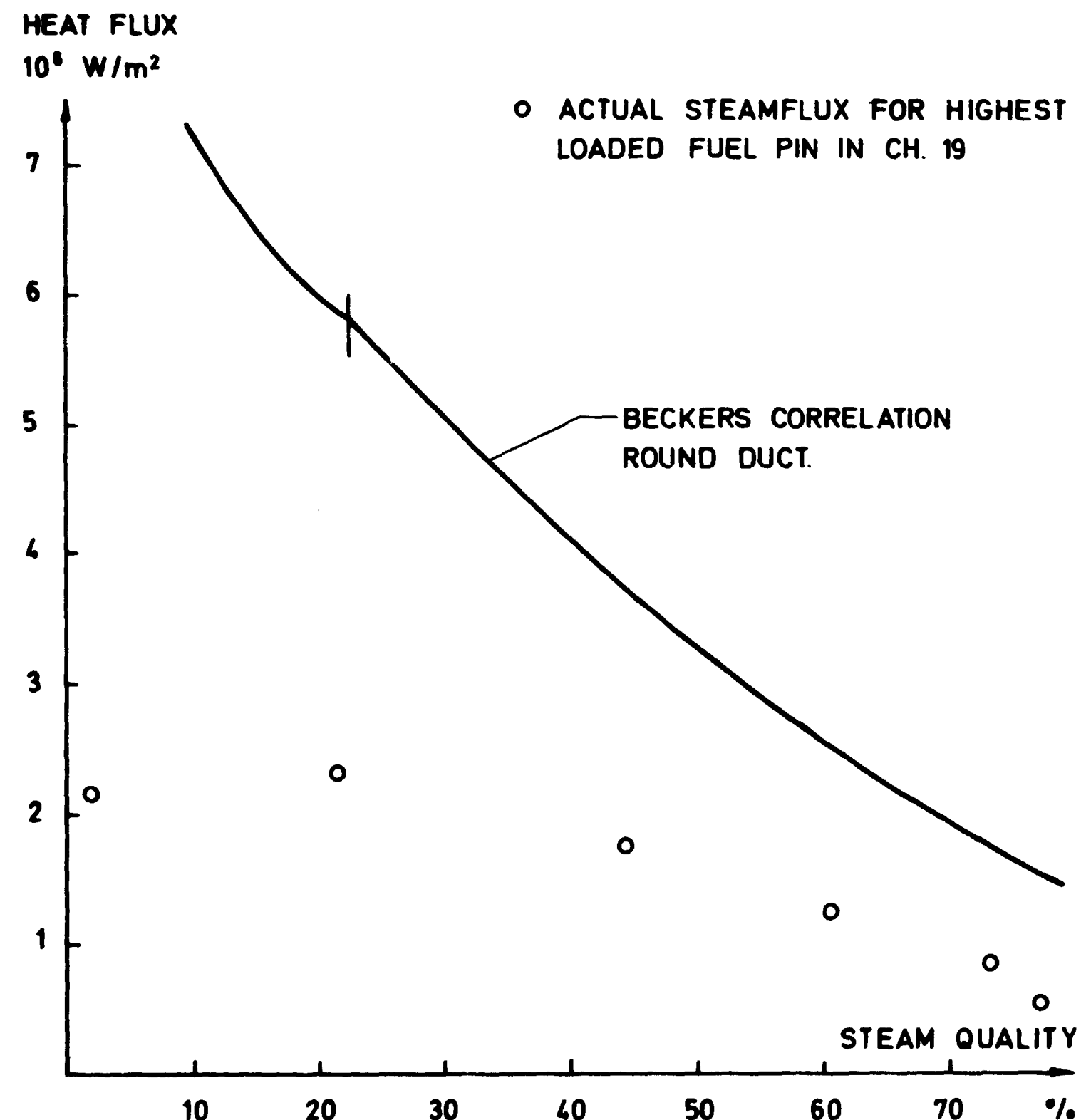


Fig. 5.3b. Burn out prediction in Dresden 1. (Channel 19).

#### 5.4. Concluding Remarks on Burn Out Calculations

The above calculations do not make it possible to draw any definite conclusions concerning burn out calculations. The prediction of burn out by means of a subchannel calculation as it is performed here is not identical to the one in ref. 18, and it might yield quite different results.

However, it still seems to be reasonable to use correlations of the Becker and GE type in connection with overall calculations to find the fuel elements which are closest to burn out and then perform a subchannel



analysis for these using power distributions from the overall calculation.

Yet, the latter method of burn out predictions, at least as it appears from open literature, still need further development.

## 6. SUMMARY AND CONCLUSIONS

The present report has summarized the features of the boiling water reactor simulator complex SYNTRONVOID, ELGYFO. The description does not include those concerning burn up and the coupling between power calculations and hydraulic calculations.

The whole of the hydraulic model is based on experimentally fitted models and correlations. The neutron flux distribution calculation is in contrast to this as far as possible based on first principles. Reasonable computing times are obtained by use of flux synthesis.

Calculations have been carried out to show some of the effects inevitable approximations will have. The effects have all been demonstrated by altering some approximation or parameter, or by comparing with some more detailed calculational method. This also includes a detailed hydraulic analysis by means of a subchannel calculation. This method of verification can show too crude approximations, but cannot finally confirm the validity of these.

Further, the calculations described do not take into account approximations in producing nuclear data.

As a last step burn out calculations by means of the Becker correlation which has been incorporated into SYNTRONVOID and ELGYFO have been demonstrated.

### 6.1. The Hydraulic Models

In terms of the power shape the hydraulic models seem to be adequate. As long as the fitted constants for the models are chosen among those which is known to fit to some experimental situation, the power shape and steam quality distribution are not changed dramatically. If the constants are fitted to experiments which are close to the actual reactor condition and geometry, the models are believed to yield good results.

Until now the computing time for the hydraulics has been satisfactory. It has been 10-20% of the total computing time for the example used in this report.

Experience with the fitting of the models also indicates that a set of more crude models might be used if additional computing speed is needed.

Speed will be gained at the expense of more fitting to a particular situation. Also for this purpose the more detailed models will be a useful tool.

### 6.2. Neutron Flux Calculation

The flux synthesis method is a very fast and valuable method as long as the reactor configuration is simple. This has been demonstrated in ref. 6.

When the geometry is complicated by different control rod setting and voids, the advantage in using flux synthesis becomes less. The number of meshes and trial functions is then increased if reasonable flux distributions should be calculated. Some flux shapes the method might even fail completely to calculate properly.

While experience rather easily shows how to select the best trial functions and mesh size for simple geometries more complicated geometries make the choice difficult. In practice such complicated situations will demand checks of different kinds either by measured values or by comparing to difference equation technique. Thus the advantage of the synthesis method to be a method needing no experimental fitting, does not always exist.

In contrast to the synthesis method, nodal theory, which is an obvious alternative, always needs fitting. On the other hand, when this has been done experience from other institutions shows that it yields satisfactory results in many cases.

The choice of synthesis or nodal theory for overall reactor calculations cannot be made beforehand. The problem in hand will determine whether one or the other is the most favourable to use.

### 6.3. Subchannel and Burn out Calculations for a BWR Fuel Element

By subchannel calculations the influence of the radial void distribution on the radial power form factor in a fuel element has been investigated. The form factor is modified by less than 5%. The effects of the non-uniform radial void distribution on the neutron spectrum seems to be negligible. The effects on the homogenized cross sections for fuel elements are thus also small.

From the literature experience indicated that the Becker burn out correlation for a fuel element included in SYNTRONVOID and ELGYFO will yield a good estimate of whether the burn out margin is exceeded or not. It should be borne in mind that estimating burn out margin demands an increased accuracy of the calculated power. The burn out condition in a BWR is essentially determined by heat flux and steam quality. Since the quality



is determined by the power, this will enter twice in the burn out calculation.

#### 6.4. Conclusion

When a reactor physics code complex is to be tested, it should be tested against experiments. However, experimental results are scarce because of the commercial value of these.

Comparisons with results from only one reactor are of very limited value because of the big number of uncertainties. As pointed out in ref. 19, one might stop too early in improving approximations or adjusting parameters. When the actual calculation fits the experimental situation, it is difficult to improve approximations. Yet, the obtained approximation does not necessarily fit the next reactor.

For overall calculations experience indicates that predicting the overall power shape with a high degree of accuracy in a reactor for which only fundamental data and geometry are known is not possible. Errors of the order of 50% might easily occur.

Some errors might in theory be eliminated by more detailed calculations. For example, the approximations originating from nodal or flux synthesis methods will disappear by using a difference equation method and a high number of mesh points. In practice this is not possible because of the very long computing time such an approach would require.

It is thus seen that reactor calculations inevitably involve fitting. It might turn out that if one is not particularly interested in design calculations, the most economic and efficient approach is to treat a program for overall calculations as a correlation fitted to the given reactor.

#### ACKNOWLEDGEMENT

The whole Reactor Physics Department at Risø is acknowledged for their valuable assistance.

The author also want to thank P. Skjerk Christensen for having performed the nodal calculation and G. K. Kristiansen for having performed the three-dimensional difference equation calculation.

#### REFERENCES

- 1) H. Larsen, SYNTRON, A Three-dimensional Flux Synthesis Programme. Risø-M-1346 (1971) 33 pp.
- 2) A. M. Hvidtfeldt Larsen, H. Larsen and T. Petersen, Calculations on a Boiling Water Reactor as a Test of the Risø Reactor Code Complex. Risø Report No. 268 (1972) 102 pp.
- 3) D. L. Delp et al., FLARE, A Three-dimensional Boiling Water Reactor Simulator. GEAP 4598 (1964) 95 pp.
- 4) P. Bakstad and K. O. Solberg, A Model for the Dynamics of Nuclear Reactors with Boiling Coolant with a new Approach to the Vapour Generating Process. KR 121 (1967) 68 pp.
- 5) O. Nylund et al., Hydrodynamic and Heat Transfer Measurements on a Full-Scale Simulated 36-Rod BHWTR Fuel Element with Non-Uniform Axial and Radial Heat Flux Distribution. The FRIGG Loop Project. FRIGG-4 (1970) 66 pp.
- 6) H. Larsen, Approximate Methods for 3D Overall Calculations on Light Water Reactors. Risø Report No. 270 (1972) 48 pp.
- 7) H. Larsen, Three-Dimensional Boiling-Water Reactor Neutron Flux Calculations on the Basis of Homogenized Fuel Box Cross Sections. Risø-M-1616 (1973) 17 pp.
- 8) Torben Petersen and Peter Kirkegaard, The Y-matrix Concept, a Method for Treating Heterogeneities in Diffusion Calculations. Risø-M-1607 (1973) 22 pp.
- 9) G. K. Kristiansen, DC4 To Day. Short Description of DC4, V2. RF-Memo-183 (1973) Internal Report.
- 10) D. Babala, N. Bech, K. Haugset et al., ANDYCAP-A Three-Dimensional Computer Programme for Transient Analysis of Boiling Water Reactors. In: Reaktortagung, Bonn, 30. März-2. April 1971. Tagungsbericht (Deutsches Atomforum E. V., Bonn, 1971) 238-240.
- 11) N. Bech, F. Cortzen, Z. Rouhani and O. Imset, A Description of the SDS Program for Subchannel Analysis. Part 1-4. Not published.
- 12) K. E. Lindstrøm Jensen, Development and Verification of Nuclear Calculation Methods for Light-Water Reactors. Risø Report No. 235 (1970) 161 pp.

- 13) L.S. Tong, **Boiling Heat Transfer and Two-Phase Flow** (John Wiley and Sons Inc., New York, 1965) 242 pp.
- 14) L.S. Tong, **An Evaluation of the Departure from Nucleate Boiling in Bundles of Reactor Fuel Rods.** Nucl. Sci. Eng. 33, (1968) 7-15.
- 15) Kurt M. Becker, **A Correlation for Burnout Predictions in Vertical Rod Bundles.** S-349 Aktiebolaget Atomenergi (1966) 24 pp.
- 16) H.S. Isbin et al., **A Model for Correlating Two-Phase, Steam-Water, Burnout Heat-Transfer Fluxes.** Heat Transfer 83, (May 1961) 149-157.
- 17) E. Janssen and S. Levy, **Burnout Limit Curves for Boiling Water Reactors.** APED-3892 (1962) 22 pp.
- 18) R. Evangelisti et al., **Heat Transfer Crisis Data with Steam-Water Mixture in a Sixteen Rod Bundle.** Int. J. Heat Mass Transfer 15 (1972) 387-402.
- 19) B. Micheelsen and H. Neltrup, **Tasks and Problems in Reactor Physics Calculations.** Risø-M-1572 (1973) 11 pp.